The action potential in mammalian central neurons

Bruce P. Bean

Abstract | The action potential of the squid giant axon is formed by just two voltage-dependent conductances in the cell membrane, yet mammalian central neurons typically express more than a dozen different types of voltage-dependent ion channels. This rich repertoire of channels allows neurons to encode information by generating action potentials with a wide range of shapes, frequencies and patterns. Recent work offers an increasingly detailed understanding of how the expression of particular channel types underlies the remarkably diverse firing behaviour of various types of neurons.

Heterologous expression
Expression of protein molecules by the injection of complementary RNA into the cytoplasm (or complementary DNA into the nucleus) of host cells that do not normally express the proteins, such as *Xenopus* oocytes or mammalian cell lines.

Spike
Another term for an action potential (especially the portion with the most rapidly changing voltage).

Harvard Medical School, Department of Neurobiology, 220 Longwood Avenue, Boston, Massachusetts 02115, USA.
e-mail: bruce_bean@hms.harvard.edu
doi:10.1038/nrn2148

In the years since the Hodgkin–Huxley analysis of the squid axon action potential[1], it has become clear that most neurons contain far more than the two voltage-dependent conductances found in the squid axon[2,3]. Action potentials serve a very different function in neuronal cell bodies, where they encode information in their frequency and pattern, than in axons, where they serve primarily to rapidly propagate signals over distance. The membrane of the squid axon is a poor encoder, as it fires only over a narrow range of frequencies when stimulated by the injection of widely-varying current levels[4]. By contrast, most neuronal cell bodies (in both vertebrate and invertebrate animals) can fire over a far wider range of frequencies and can respond to small changes in input currents with significant changes in firing frequency[5–10]. Clearly, this richer firing behaviour depends on the expression of more types of voltage-dependent ion channels. Interestingly, although the squid axon is strikingly deficient as an encoder, some other invertebrate axons can fire over a wide frequency range[11] and have a richer repertoire of ion channel types[12], as do at least some mammalian axons[13].

The presence of multiple channel types in most neurons has been appreciated since at least the 1970s. However, few were prepared for the staggering number of distinct kinds of ion channels revealed over the last two decades by the convergent techniques of patch-clamp recording, heterologous expression of cloned channels and genomic analysis — including, for example, more than 100 principal subunits of potassium channels[14]. Even more surprising, perhaps, was the gradual realization of just how many distinct voltage-dependent conductances are expressed by individual neurons in the mammalian brain — commonly including 2 or 3 components of sodium current, 4 or 5 different components of voltage-dependent calcium currents, at least 4 or 5 different components of voltage-activated potassium current, at least 2 to 3 types of calcium-activated potassium currents, the hyperpolarization-activated current I_h, and others. Because of this complexity, our understanding of how different conductances interact to form the action potentials of even the best-studied central neurons is still incomplete, even though Hodgkin and Huxley devised the basic experimental approach still being used — voltage-clamp analysis of individual time- and voltage-dependent conductances and reconstruction of the whole by numerical modelling — more than half a century ago[1]. In this review I discuss differences in the shape, rate and pattern of firing of action potentials between various types of neurons, focusing on mammalian central neurons, and review recent advances in understanding the role of specific types of ion channels in generating these differences.

All spikes are not alike

The shape of action potentials (BOX 1) differs considerably among various types of neurons in the mammalian brain (FIG. 1). For example, in the cortex and hippocampus, GABA (γ-aminobutyric acid)-releasing interneurons generally have narrower spikes than glutamatergic pyramidal neurons. This is seen most clearly in intracellular recordings, in which spike shape can be determined precisely[8,15,16] (FIG. 1), but the difference in spike width is also evident from extracellular recordings *in vivo*[17]. Cells with narrow spikes also commonly (but not always[8]) display 'fast-spiking' behaviour: being capable of firing at high frequencies with little decrease in frequency during prolonged stimulation[5,6,8,9,15,18–20]. Recently, the fast-spiking phenotype has been related to expression of the Kv3 family of voltage-gated potassium

Projection neurons
Neurons with relatively long axons that project out of a local circuit (distinct from interneurons).

Bursting
The firing of a rapid series of several action potentials with very short (less than ~5 ms) interspike intervals.

Adaptation
Slowing or cessation of firing during a maintained stimulus.

Initial segment
The slender initial region of an axon where it originates from an axon hillock of the cell body (or sometimes from a major dendrite), characterized by the fasciculation of microtubules.

Box 1 | **Anatomy of an action potential**

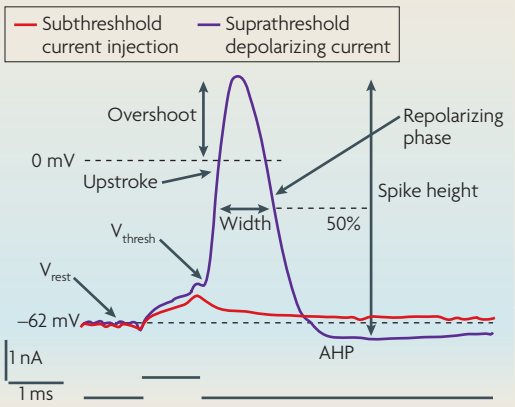

The figure shows an action potential recorded from a pyramidal neuron in the CA1 region of a rat hippocampus[117], illustrating commonly measured parameters. The action potential was elicited by the injection of just-suprathreshold depolarizing current (purple). Use of a brief (1 ms) injection has the advantage that the spike and the afterpotentials are not directly influenced by the current injection. The response to a subthreshold current injection is also shown (red). Resting potential (V_{rest}) is typically in the range of –85 mV to –60 mV in pyramidal neurons. Voltage threshold (V_{thresh}) is the most negative voltage that must be achieved by the current injection for all-or-none firing to occur (in this neuron it is about –53 mV, a typical value). Threshold is less well defined for spontaneously firing neurons, especially in isolated cell bodies where transition from gradual interspike depolarization to spike is typically less abrupt than in slice recordings, and for such cases threshold is more easily estimated from phase-plane plots (FIG. 2). The upstroke (also called the depolarizing phase or rising phase) of the action potential typically reaches a maximum velocity at a voltage near 0 mV. Overshoot is defined as peak relative to 0 mV. Spike height is defined as the peak relative to either resting potential or (more commonly) the most negative voltage reached during the afterhyperpolarization (AHP) immediately after the spike. Spike width is most commonly measured as the width at half-maximal spike amplitude, as illustrated. This measurement is sometimes referred to, confusingly, as 'half-width' or 'half-duration'; 'half-height width' would be clearer. As is typical for pyramidal neurons, the repolarizing phase (also called 'falling phase' or 'downstroke') has a much slower velocity than the rising phase. Figure modified, with permission, from REF. 117 © (1987) Cambridge Univ. Press.

channels, the rapid and steeply voltage-dependent activation and deactivation kinetics of which are well-suited for generating narrow action potentials and short refractory periods[6,21–27]. The fast-spiking phenotype is not confined to interneurons, since Purkinje neurons (which are GABAergic projection neurons) also fire steadily at high frequencies and have narrow action potentials that are repolarized mainly by Kv3-mediated currents[28–31]. Nor are all fast-spiking neurons GABAergic, as neurons of the subthalamic nucleus, which are glutamatergic, have this phenotype[7,32] and express large potassium currents mediated by Kv3-family channels[33]. The calyx of Held, a presynaptic glutamatergic terminal, also has narrow spikes with repolarization by Kv3 channels and can fire at high frequencies[34–36].

The distinctive phenotype of fast-spiking neurons with narrow action potentials is unusual in that it presents a general correlation across many neuronal types between firing behaviour and action potential shape. In general, however, firing behaviour can take many different forms of patterns and frequencies, with little obvious correlation with spike shape[8,15,37,38]. The firing pattern of a neuron (which includes frequency of firing as a function of stimulus strength, bursting versus non-bursting activity and adapting versus non-adapting behaviour) is probably a more important physiological property than the shape of the spike. However, the two cannot be cleanly separated, as differences in ionic conductances producing differences in firing patterns will in general also produce differences in spike shape, although these may be more subtle. Spike shape *per se* is probably most significant at presynaptic terminals, where small differences in shape can produce changes in the timing of presynaptic calcium entry, leading to dramatic changes in postsynaptic currents. Interestingly, spike shape in presynaptic terminals can be quite different to that in the cell body of the same neuron[39] (FIG. 1f,g).

Somatic versus membrane action potentials

The Hodgkin–Huxley analysis of the squid axon action potential[1] was greatly facilitated by creating an artificial situation in which all of the axonal membrane experiences the same voltage at the same time — the 'membrane action potential' — which is achieved by inserting an axial wire to make axial resistance negligible. In mammalian neurons, action potentials are usually recorded from cell bodies in brain slices, in which axons and dendritic trees are largely intact. In this situation, the cell body is roughly isopotential during the spike (that is, the membrane voltage is the same at different places and undergoes simultaneous change), but there may be current flow between the cell body and the dendrites and axon of the cell that alters the shape of the action potential to some extent. In most central neurons, the spike appears to be initiated in the initial segment of the axon[40–47], at a location that in pyramidal neurons is typically 30–50 µm from the cell body. This is far enough away that the shape of the action potential recorded in the cell body can show clear effects arising from non-uniformity of voltage[40,41,47]. Dendrites probably also influence the form of somatically recorded action potentials, partly by serving as a capacitative load that slows and truncates fast spikes (by absorbing currents that would otherwise go to changing somatic voltage) but also by playing an active part in generating afterdepolarizations. Thus, although the action potential recorded in the cell body of a neuron in a brain slice preparation is much closer to a membrane action potential than to a uniformly propagating axonal action potential, non-uniformity of voltage can be significant, especially when it is changing most rapidly.

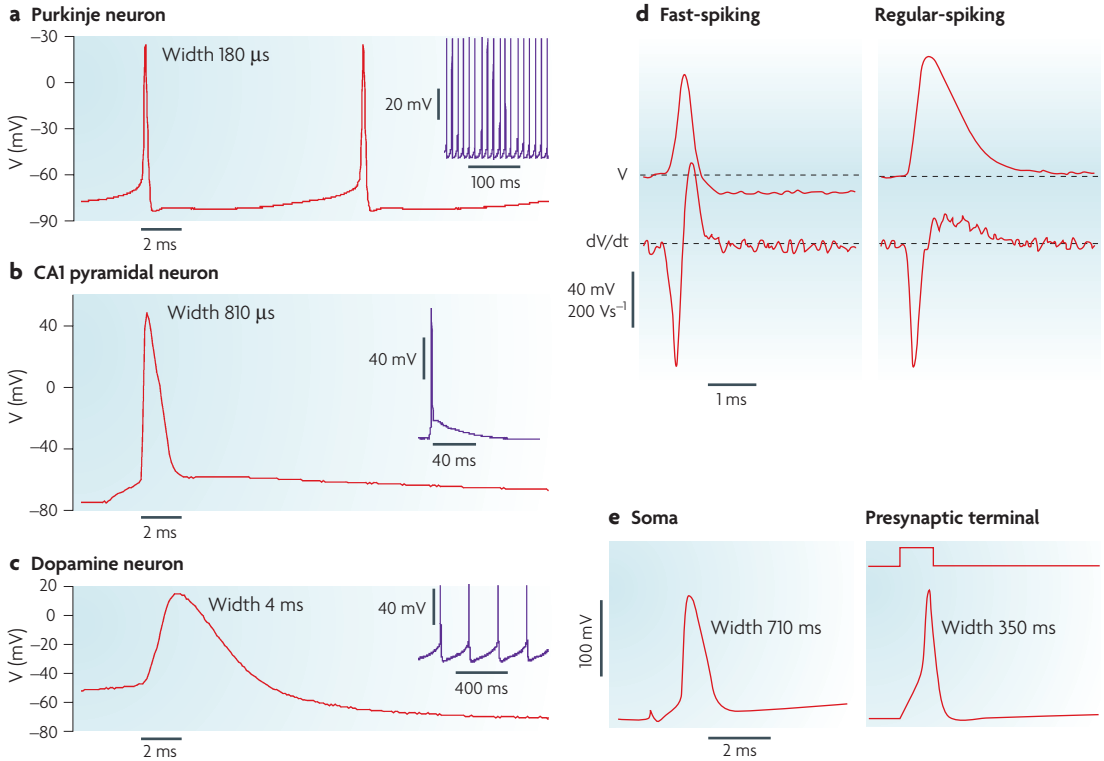

Figure 1 | **Diversity of action potentials in central neurons. a** | Spontaneous action potentials in an acutely dissociated mouse cerebellar Purkinje neuron (A. Swensen, unpublished observations). **b** | Action potential in a hippocampal CA1 pyramidal neuron in brain slice (M. Martina, unpublished observations). **c** | Spontaneous action potentials in a midbrain dopamine neuron (M. Puopolo, unpublished observations). Note the dramatic differences in width between these three action potentials. **d** | Illustration of action potentials from fast-spiking and regular-spiking cortical neurons. Note the faster repolarization rate in the narrow spike of the fast-spiking neuron. V is membrane voltage, and dV/dt is the time derivative of membrane voltage. The signal in extracellular recordings is essentially proportional to dV/dt, and spike widths can be measured from the distance between the peaks in the dV/dt signal. **e** | Different action potential widths in the soma of dentate gyrus granule neurons and in the mossy fibre bouton, a presynaptic terminal made by a granule neuron. Note the narrower action potential in the presynaptic terminal compared to the soma. Panel **d** reproduced, with permission, from REF. 15 © (1985) American Physiological Society. Panel **e** reproduced, with permission, from REF. 39 © (2000) Elsevier Science.

To analyse the ionic currents flowing during action potentials, a particularly useful preparation is provided by acutely dissociated cell bodies, in which action potentials are close to true membrane action potentials and where high-resolution voltage-clamp experiments — including action potential clamp experiments (BOX 2) — can be performed on the same cell in which the action potential is recorded (FIGS 2c,d; 3a–c). Typically, acutely dissociated neurons include a stump of axon as well as varying amounts of proximal dendrites, but the remaining processes are usually short enough that the whole membrane surface is likely to be nearly isopotential, even during spikes. Many neurons, including Purkinje neurons[48], hippocampal pyramidal neurons[49,50], neurons from deep cerebellar nuclei[51], subthalamic nucleus neurons[32], striatal medium spiny neurons[52], globus pallidus neurons[53] and midbrain dopamine neurons[54] (FIG. 2a,b) have action potential shapes and firing properties when dissociated that appear to be very similar to those of the same neuronal type in brain slices. For example, dissociated cerebellar Purkinje neurons fire spontaneously, with typical frequencies near 40 Hz, and also form all-or-none bursts of action potentials when stimulated from hyperpolarized voltages[48,55], similar to the behaviour of intact neurons in brain slices[56,57].

A simple but remarkably informative way of examining the properties of action potentials is to plot the time derivative of the voltage (dV/dt) versus the voltage: a so-called phase-plane plot[58] (FIG. 2a–b). Information about the time course of the spike is lost, but some aspects of the spike are clearer than in a simple display of voltage versus time. For example, the spike threshold is immediately evident as being the voltage at which dV/dt increases suddenly. A particular utility of phase plane plots comes from the relationship between dV/dt and membrane current. For a membrane action potential under conditions of no current injection, ionic current through the membrane (the net current through all channels) is equal and opposite to the capacitative current (since ionic current can go nowhere except to charge or discharge the membrane capacitance). This is expressed in the equation $I_{ionic} = -CdV/dt$, where I_{ionic} is the net ionic current, C is the cell capacitance and dV/dt is the time derivative of voltage[59]. As cell capacitance

Node of Ranvier
Interruption of the myelin sheath in a myelinated nerve fibre.

Outside-out patch
A variant of the patch-clamp technique in which a patch of plasma membrane covers the tip of the electrode, with the outside of the membrane exposed to the bathing solution.

Activation
Conformational change of a channel molecule from a closed (non-conducting) to an open (conducting) state (for voltage-dependent channels, this is usually by depolarization of the membrane).

is an easily measured parameter, the phase plane plot for a membrane action potential gives a direct read-out of net ionic current as a function of voltage during the various phases of the action potential. For example, the maximum sodium current flowing during the spike can be estimated from the maximum CdV/dt reached during the upstroke, when contributions from other channels are likely to be small.

Interpretation of the phase-plane plot for an action potential recorded in the cell body of an intact neuron is more complicated than for a membrane action potential, as the presence of a dendritic tree and axon means that not all ionic current goes to charge or discharge the somatic membrane. In their classic examination of action potentials in spinal motor neurons, Coombs and colleagues[40] observed that the main spike was preceded by a smaller, earlier component (more recently called 'the kink'[47]). This component was interpreted as reflecting initiation of the spike in the initial segment of the axon. Such a component is seen in somatic spikes recorded from a wide variety of central neurons[41,47,60] (FIG. 2a), and direct simultaneous intracellular recordings in pyramidal neurons have confirmed that the spike occurs in the initial segment of the axon before the somatic spike[43,45,47]. The possibility that the spike may occur first even farther from the soma, in the first node of Ranvier, has also been considered[60,61], but at least in cerebellar Purkinje neurons and layer 5 cortical pyramidal neurons the weight of evidence supports initiation in the initial segment[45,46]. In Purkinje neurons, blocking sodium entry at the first node of Ranvier has no effect on the somatic spike waveform (including the kink), whereas inhibiting sodium entry at the initial segment reduces the kink[46].

Box 2 | **Action potential clamp and dynamic clamp**

The contribution of particular currents to the action potential — the 'internal anatomy' of a spike — can be dissected using the action potential clamp technique (FIGS 2,3,5), in which the cell is voltage-clamped using a previously-recorded action potential waveform as the command voltage[110], ideally recorded minutes earlier in the same neuron. The ion channels experience precisely the same trajectory of voltage as during a naturally occurring action potential, and thus each component of current flows with exactly the same time course and size. Individual components of current can be isolated using specific blockers or changes in ionic composition — without changing the voltage trajectory, as occurs when blocking conductances in a current clamp. Accurate measurement of the large, fast currents during the spike requires a fast, spatially uniform voltage clamp, which is possible with acutely isolated cell bodies or outside-out patches. Smaller currents preceding and following the spike can be studied in whole-cell brain slice recordings[54].

Whereas the action potential clamp technique directly measures various currents during normal spiking, the ingenious dynamic clamp technique[198–200] instead examines how spiking is changed by adding, removing or altering the kinetics of particular currents. The effect of adding or removing a conductance on firing in current clamp recordings is simulated by calculating in real time the current that would be produced by the artificial conductance and injecting that current. For voltage- and time-dependent conductances like those underlying the action potential, equations accurately describing the voltage- and time-dependence are needed, and these must be numerically integrated in real time. Update rates up to 50 kHz are possible[26,200], and are adequate for simulating conductances during the spike. Often, relatively non-selective blockers are used to block multiple conductances (for example, tetraethylammonium ion or 4-aminopyridine, which generally block multiple types of potassium channels), and the effect of adding back a particular simulated conductance is tested.

Sodium currents during action potentials

The main contribution of voltage-dependent sodium channels to the action potential is explosive, regenerative activation of inward current during the rising phase[1]. Detailed measurements of sodium current in acutely dissociated cell bodies or outside-out patches of central neurons[48,62–65] show gating properties generally similar to those in squid axons[66,67], with current activating rapidly (hundreds of microseconds) and inactivating with a time constant of less than a millisecond for depolarizations beyond 0 mV. However, the kinetics of sodium currents differ in detail between different types of neurons[62] and, remarkably, even between different regions of the same neuron, with sodium channels in hippocampal mossy fibre boutons (formed by the axons of granule cells of the dentate gyrus) inactivating twice as fast as the sodium channels in the granule cell somata[68]. The molecular basis of these differences is not yet known. The wider action potentials in granule cell bodies (680 µs at half-height) compared to those in mossy fibre boutons (380 µs at half-height)[39] (FIG. 1f,g) could result partly from slower repolarization due to slower-inactivating sodium current continuing to flow during the falling phase of the spike. However, potassium currents may also differ between the two cell regions.

It has recently been reported that sodium currents in mammalian central neurons activate upon step depolarizations with much less delay than is predicted by the Hodgkin–Huxley model, in which activation of sodium current has a sigmoid time course, described by a variable following first-order kinetics raised to the third power ('m^3' kinetics). By contrast, Baranauskas and Martina[65] found that sodium currents in central neurons activate with even less sigmoidicity than predicted by m^2 kinetics[65]. The report's description is consistent with previous studies in other vertebrate sodium channels: when sodium current activation in the frog or rat node of Ranvier was fitted with m^n kinetics, n varied from less than 2 for small depolarizations (where the measurements of Baranauskas and Martina were made) to 4 for large depolarizations[69,70]. These results should prompt a close examination of the kinetics of cloned sodium channels in heterologous expression systems, which avoid complications from the overlap of multiple currents from the multiple sodium channel types probably present in central neurons.

A much more radical proposal concerning sodium channel kinetics in central neurons was recently made: that there is cooperativity between neighbouring sodium

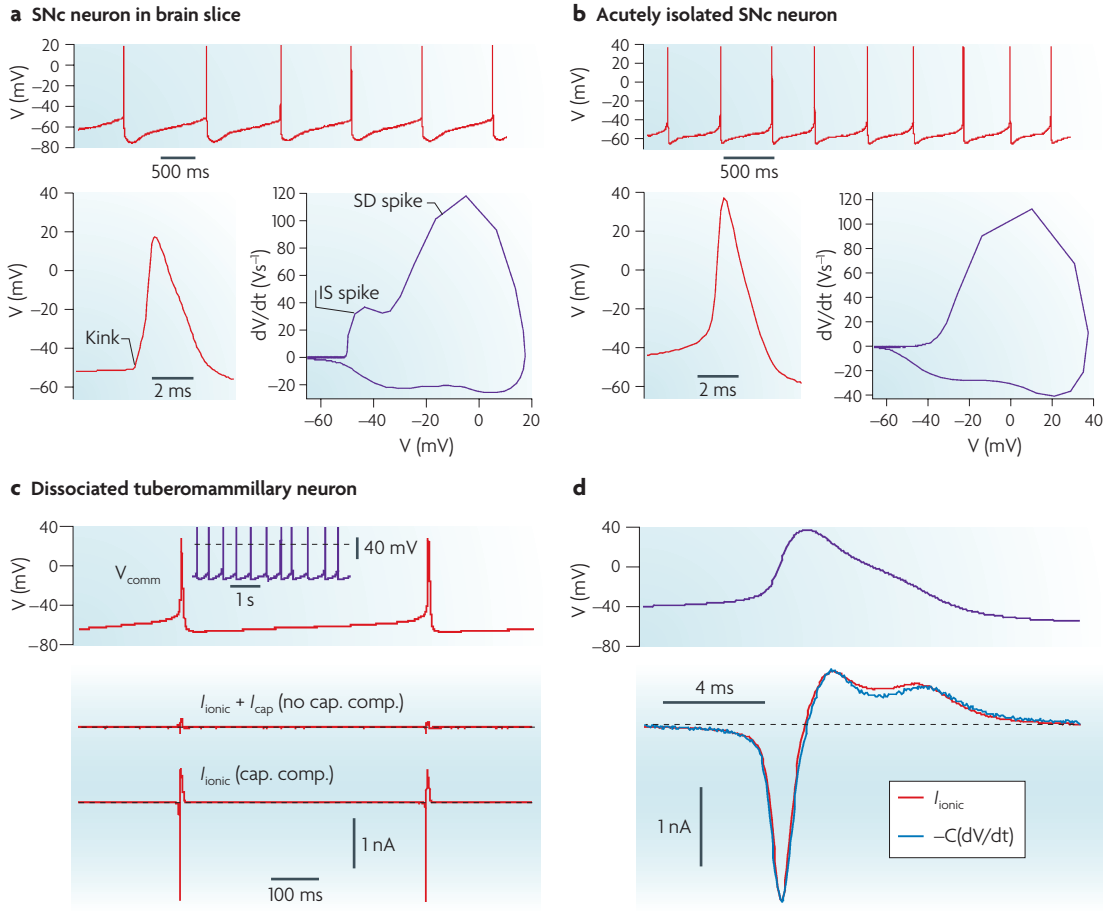

Figure 2 | **Phase-plane plots and action potential clamp. a** | Pacemaking activity recorded from a dopaminergic neuron in the substantia nigra pars compacta (SNc) of a mouse brain slice (M. Puopolo, unpublished observations). Bottom left, action potential at higher resolution, illustrating abrupt rise (kink). Bottom right, phase plane plot, illustrating the distinct components reflecting initiation in the initial segment (IS) and subsequent somatic dendritic (SD) spike[40–42]. **b** | Pacemaking activity in an acutely dissociated dopaminergic neuron (M. Puopolo, unpublished observations). Note lack of kink and IS component. **c** | Action potential clamp (BOX 2) in a dissociated neuron from the tuberomammillary nucleus. Spontaneous action potentials were recorded in current clamp mode (the upper purple trace shows a 5-second segment of spontaneous firing) and then used as the command voltage (V_{comm}) after switching the amplifier to voltage-clamp mode. With no compensation for cell capacitance (no cap. comp., lower panel, upper trace), recorded total current is nearly zero (since ionic (I_{ionic}) and capacitative (I_{cap}) currents are equal and opposite during spontaneous action potentials recorded with no current injection). Ionic current was measured after analogue compensation for the cell capacitance (34 pF) (cap. comp., lower panel, lower trace). **d** | Comparison of the net ionic current (red trace) measured in voltage clamp mode using the action potential waveform (upper purple trace) as the command voltage with predicted ionic current calculated from the voltage waveform as –CdV/dt (blue trace), where C is cell capacitance. Note the shoulder in the action potential associated with an inflection in outward current during repolarization. V, membrane voltage. Panels **c**,**d** modified, with permission, from REF. 98 © (2002) Elsevier Science.

Subthreshold voltages
Voltages negative to the threshold voltage (BOX 1) for action potential firing (which is typically in the range of –55 mV to –40 mV in mammalian central neurons).

Tetrodotoxin
(TTX). Alkaloid toxin derived from *Fugu* puffer fish that is a potent and highly selective blocker of voltage-dependent sodium channels.

Inactivation
Conformational change of a channel molecule to a closed state that differs from the closed 'resting' state in that the channel cannot be opened (for example, by further depolarization).

channels such that the opening of channels shifts the activation curves of neighbouring channels in the hyperpolarized direction[71]. This proposal aimed to account for an abrupt initial rising phase of the action potential, which is seemingly incompatible with predictions of m^3 kinetics, along with trial-to-trial fluctuations in the apparent threshold voltages. The hypothesis of cooperativity among neighbouring channels might best be tested in nodes of Ranvier, where sodium channel density is extremely high and good voltage clamp is possible. Most likely, however, the observed abrupt initial rising phase of the action potential (recorded from cell bodies in slices) simply results from the kink reflecting initiation of the spike in the initial segment[40,47,72]. Apparent variability in threshold can be explained by instantaneous differences between subthreshold potentials in the cell body and the initial segment[72]. Thus, while sodium channel kinetics near threshold may be less sigmoid than Hodgkin–Huxley predictions, the hypothesis of cooperative gating among sodium channels seems unnecessary.

In some central neurons, specialized kinetics of sodium currents give rise to a component of tetrodotoxin (TTX)-sensitive sodium current immediately after the spike. This is the 'resurgent' sodium current, which activates transiently upon repolarization following inactivation by strong depolarizing pulses[48,73]. This current appears to

arise from an unusual mechanism of inactivation: channels are plugged by a positively charged intracellular blocking particle (probably the cytoplasmic tail of the β4 sodium channel subunit[74]) after they open. On repolarization, the block is relieved, and the channels carry an inward sodium current transiently before deactivating[48,73,74]. Recovery from inactivation occurring by this mechanism is faster than recovery from normal inactivation[73], so that as sodium channels pass depolarizing resurgent sodium current after a spike, they also recover from inactivation, producing a pool of channels that are available to give transient sodium current upon depolarization. Both effects promote faster firing of a second spike.

Resurgent current has been found in cerebellar Purkinje neurons[48], cerebellar granule neurons[75,76], neurons in the deep cerebellar nuclei[51,75], cerebellar unipolar brush cells[75], motor neurons of the trigeminal mesencephalic nucleus[77], neurons from the medial nucleus of the trapezoid body[78] and subthalamic nucleus neurons[32], as well as in a subset of neurons in dorsal root ganglia[79]. Consistent with its 'anti-refractory' properties, the presence of resurgent current appears to be generally correlated with the ability of cells to fire rapidly and, at least in the case of Purkinje neurons, to generate bursts[48,80]. It is not yet clear whether a resurgent sodium current is present in all fast-firing cells; fast-spiking interneurons are a case of particular interest not yet examined.

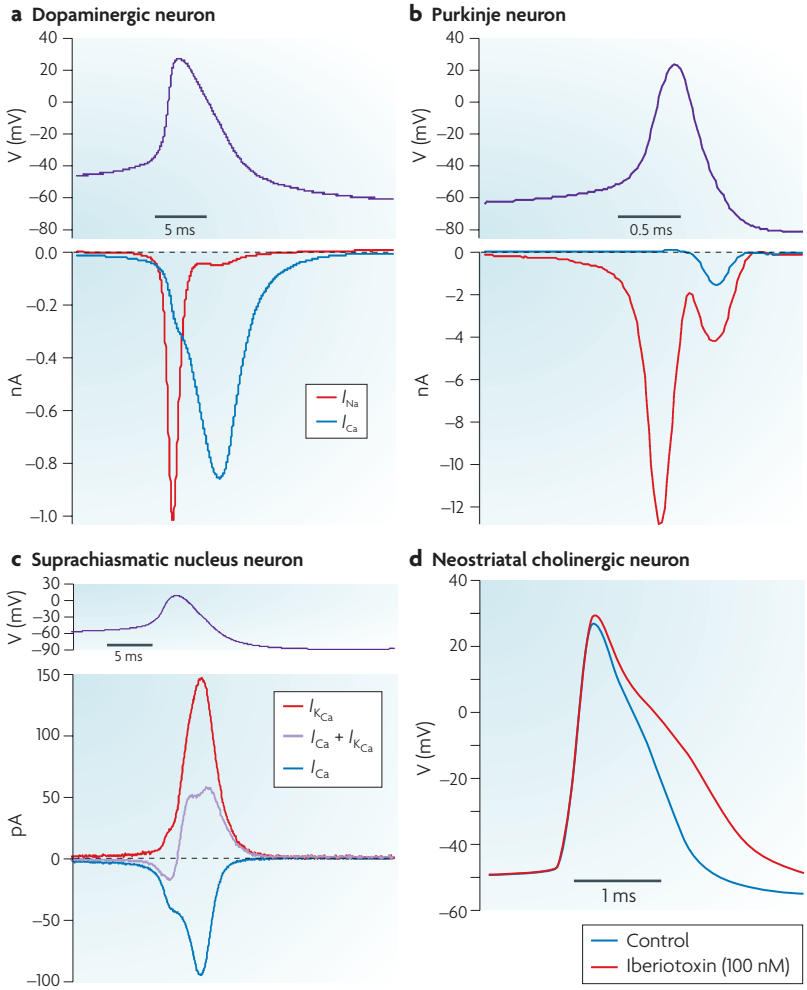

Figure 3 | **Sodium, calcium, and calcium-activated potassium currents during action potentials.** Sodium current (I_{Na}, red) and calcium current (I_{Ca}, blue) in a midbrain dopaminergic neuron (**a**) and a cerebellar Purkinje neuron (**b**), recorded using the action potential clamp technique (B. Carter, unpublished observations). Purple traces show recorded spontaneous action potentials used as command voltages. Block by tetrodotoxin (1 μM) defined the sodium current. Calcium current was determined by replacing calcium by cobalt (in the dopaminergic neuron) or by magnesium (in the Purkinje neuron), in the presence of 5 mM tetraethylammonium chloride to block large conductance calcium-activated potassium (BK) current ($I_{K_{Ca}}$). Note the different timescales. The calcium currents are of a similar magnitude, whereas the sodium current in the Purkinje neuron is much larger than the other currents (so large that voltage clamp is probably imperfect due to series resistance errors). The time course and magnitude of calcium current (blue) and calcium-activated potassium current (red) in a spontaneous action potential of a suprachiasmatic nucleus (SCN) neuron can be seen in panel **c**. Net current resulting from calcium entry is outward except at the beginning of the spike. Calcium current in SCN neurons is unusual in activating significantly during the rising phase of the spike (although still greatly outweighed by sodium current, not shown). The role of BK-mediated calcium-activated potassium current in repolarization of the action potential in a cholinergic neuron from the neostriatum is revealed by the effect of iberiotoxin, a specific blocker (**d**). V, membrane voltage. Panel **a** modified, with permission, from REF. 54 © (2007) Society for Neuroscience. Panel **c** modified, with permission, from REF. 109 © (2004) Society for Neuroscience. Panel **d** modified, with permission, from REF. 97 © (2000) Society for Neuroscience.

Calcium currents during action potentials

Mammalian neurons typically express multiple types of voltage-dependent calcium channels, and these have important roles in determining action potential shapes and firing patterns (in addition to producing the action potential-evoked increases in intracellular calcium used for intracellular signalling). Individual neurons commonly express at least 4 or 5 distinct types of calcium channels, including low-voltage-activated T-type channels (Cav3 family channels) and high-voltage-activated channels that include L-type (Cav1.2 and Cav1.3), P/Q-type (Cav2.1), N-type (Cav2.2) and R-type (Cav2.3) channels. Calcium currents generally make little contribution to the rising phase of action potentials because their activation kinetics are slower than sodium channels. Calcium channels typically begin to be activated near the peak of the action potential and calcium currents are largest during the falling phase, when channels have been opened and the driving force on calcium increases (FIG. 3a,b). Interestingly, although the action potentials of virtually all neurons probably have large inward calcium currents flowing during the falling phase, blocking calcium channels often results in a broadening of the action potential[81–88] (FIG. 3d), which is opposite to the effect expected from blocking entry of positively charged ions. This reflects powerful and rapid coupling of calcium entry to the activation of large conductance calcium-activated potassium channels (BK channels), so that the net effect of blocking calcium entry is to inhibit a net outward current rather than a net inward current — that is, the potassium flux triggered by the calcium entry outweighs the calcium entry itself (FIG. 3c). The contribution of BK channels is typically greatest in the later stages of the repolarization phase[83,89,90]. Biochemical data, experiments with intracellular calcium buffers, and single channel recordings all suggest that this tight coupling reflects colocalization of

4-aminopyridine
Potassium channel blocker that inhibits some potassium channels (including Kv3 family channels and a subset of Kv1 family subunits) with a high relative potency and others (such as Kv4 channels) more weakly, or not all.

Tetraethylammonium ion
(TEA). When applied externally, this blocks some types of voltage-activated potassium channels (notably BK and Kv3 family channels) and not others.

calcium channels and BK calcium-activated potassium channels[91–96]. BK channels can apparently be colocalized in macromolecular complexes with multiple types of calcium channels, including Cav1.2, Cav2.2 and Cav2.1 channels[95].

Neurons that secrete modulatory transmitters such as noradrenaline, serotonin, dopamine, acetylcholine and histamine frequently generate broad action potentials, often with a 'shoulder' in the falling phase (FIGS 1c,2d) that appears to be due to the activation of calcium channels[97,98]. Cells with a shoulder do not necessarily have larger calcium currents during the action potential: cerebellar Purkinje neurons, with exceptionally narrow action potentials and no shoulder, actually have larger calcium currents during repolarization than midbrain dopaminergic neurons, which have broad action potentials with a prominent shoulder (FIG. 3a,b). The difference is presumably in the size and speed of opposing potassium currents, including BK calcium-activated potassium currents, which are very large in Purkinje neurons.

Activation of small conductance calcium-activated potassium channels (SK channels) is also coupled to calcium entry through multiple different types of calcium channels, including Cav2.1, Cav2.2, Cav2.3 and Cav3 family channels, with different specificity of coupling in different types of neurons[88,93,99–104]. However, so far there is no clear biochemical evidence for colocalization of SK channels with calcium channels in macromolecular complexes, and activation of SK channels (unlike activation of BK channels) can often be disrupted by the slow calcium buffer EGTA[99,105], suggesting that they are activated by calcium diffusing over longer distances. Typically, SK current is activated more slowly than BK current and contributes little to the fast repolarization phase of the action potential, but rather helps shape the afterhyperpolarization that follows. The duration of SK conductance following a spike probably reflects the decay of intracellular free calcium, with a typical time course of hundreds of microseconds. By contrast, BK channels deactivate far more quickly, since depolarization as well as high local intracellular calcium is required for activation to be maintained. In several types of pacemaking neurons, block of SK channels has the striking effect of producing substantially less regular firing[10,97,103,106,107]. Although the activation of SK channels is not as rapidly coupled to calcium entry as BK channel activation, coupling is still highly efficacious in that block of calcium entry can produce a net depolarization of the membrane potential between spikes in spontaneously active neurons[108,109], probably reflecting effects on SK rather than BK channels.

Because activation and deactivation kinetics of calcium channels are strongly voltage-dependent, action potential-evoked calcium entry can have a steep dependence on action potential width and shape. This sensitivity is especially significant in presynaptic terminals, where modest changes in action potential shape can translate into significant changes in calcium entry and even more dramatic changes in transmitter release[36,39,110–114].

Potassium currents during action potentials

Most central neurons express such a large variety of voltage-dependent potassium currents that separating and characterizing all the components of total potassium current elicited in voltage-clamp experiments by step depolarizations is daunting (and even mastering the terminology used to name them can be challenging). However, typically only a fraction of the various voltage-dependent potassium currents present in a neuron is significantly activated during normal action potentials. In addition to the BK calcium-activated potassium channels discussed above, two other classes of potassium channels that commonly contribute to spike repolarization in cell bodies are Kv4 family channels, which mediate A-type current (I_A), and Kv3 family channels.

In some fast-spiking neurons, such as cerebellar Purkinje neurons, Kv3-mediated current seems to constitute virtually all of the voltage-dependent potassium current flowing during spike repolarization[23,31]. In most of these cases, other types of potassium channels are present in the membrane, but the activation of the Kv3-mediated currents is so much faster that they activate and repolarize the spike before other potassium channels can activate significantly. The potassium current flowing during the spike may be only a small fraction of the current that can be evoked by a longer depolarizing step (FIG. 4a), providing a powerful feedback element to keep spikes narrow (since any small increase in width would produce more activation of available current).

The functional significance of Kv3 channels in the fast-spiking phenotype is highlighted by the effects of blocking the channels (with low concentrations of 4-aminopyridine (FIG. 4a,d) or tetraethylammonium ion (TEA) (FIG. 4c)), which often results in the slowing of high-frequency firing[6,26,27,35,115] (FIG. 4c,d). It is counterintuitive that removing a potassium conductance would decrease the excitability of a neuron. The reasons for this are not clear but they almost certainly involve changes in the activation of other channels secondary to the changes in spike waveform produced by block of Kv3 current. For example, a smaller afterhyperpolarization (FIG. 4c,d) might result in slower recovery from inactivation of sodium channels, or broadening of spikes might activate types of potassium channels not activated by normal narrow spikes[115]. If these channels deactivate more slowly, they could retard firing of a subsequent action potential. In fast-spiking hippocampal oriens-alveus interneurons, Lien and Jonas[26] found that when dynamic clamp was used to add Kv3-like currents back to neurons in which native currents were pharmacologically blocked, the restored currents produced faster spiking only if the deactivation rate was near that of native channels in the neurons, neither faster nor slower[26] (FIG. 4). The reasons for this remarkable tuning are not clear, but must involve complex interactions with other channels mediated by changes in spike shape. In Purkinje neurons, it has been proposed that the shape of the repolarization waveform produced by Kv3 currents leads to enhanced activation of post-spike resurgent sodium current[116].

In glutamatergic neurons in the hippocampus and cortex, at least three types of potassium currents have major roles in action potential repolarization: two types of purely voltage-dependent potassium currents, known as I_A and I_D, and BK calcium-activated currents[50,89,117–126]. The term 'I_A' has been used broadly to refer to potassium currents showing relatively rapid inactivation. In cell bodies and dendrites, the current called I_A is formed primarily by Kv4 family channels[125–127]. Kv1 family channels that include Kv1.4 subunits or the β-subunit Kvβ1 can also mediate an inactivating current that has been called I_A[14], which appears to be prominently expressed in at least some presynaptic terminals[39,128]. The term 'I_D' also has some ambiguity. The term was originally introduced to denote a 'delay' current in hippocampal pyramidal neurons that prolongs the approach to threshold[129]. This current is activated by subthreshold depolarizations, inactivates slowly, and is blocked by low concentrations (10–100 μM) of 4-aminopyridine. Dendrotoxin, which is selective for a subset of Kv1 family subunits, blocks a current with these properties[122,130], and 'I_D' is now often used to denote dendrotoxin-sensitive current. However, dendrotoxin generally has little[38] or no[131,132] effect on spike width, while low concentrations of 4-aminopyridine have a greater effect[19,50,117,119,122,131,133]. The effects of low concentrations of 4-aminopyridine on spike width in pyramidal neurons have often been ascribed to block of I_D, but in retrospect these effects may also represent block of other currents, possibly mediated by Kv3 family channels[22] or Kv1.5 channels, which are blocked by low concentrations of 4-aminopyridine but not dendrotoxin.

In a number of neurons, the action potential becomes broader in response to increased frequency of firing because of the cumulative inactivation of potassium channels. A particularly well-studied example occurs in the neuron R20 of the mollusc *Aplysia*, where frequency-dependent broadening of the action potential produces facilitation of synaptic transmission[134].

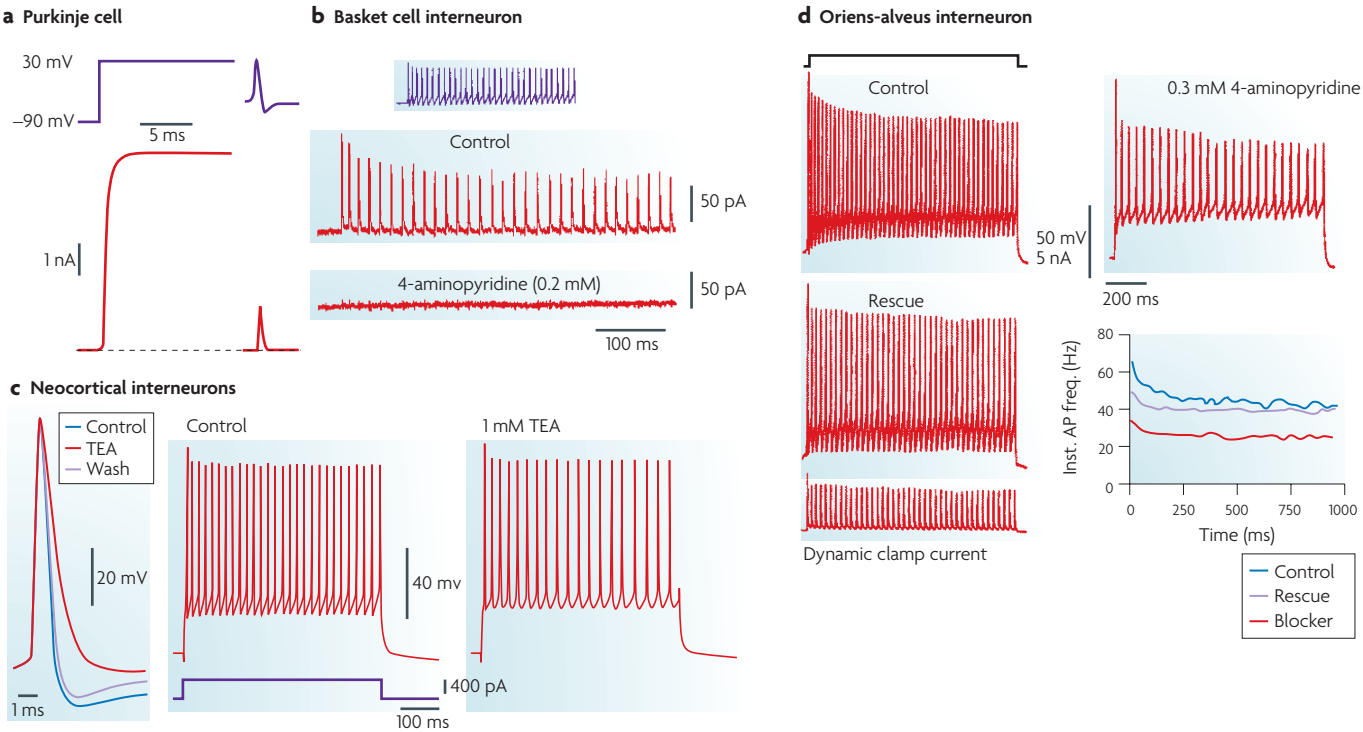

Figure 4 | **Role of Kv3 potassium currents in fast-spiking neurons. a** | Potassium currents in a nucleated patch from a Purkinje neuron elicited by a step to +30 mV and by an action potential waveform. Spike-evoked current is only a small fraction of total available current (which is almost all Kv3-mediated[28]). Any small increase in spike width can activate more current; this keeps the spikes narrow. **b** | In a nucleated patch from a dentate gyrus basket cell interneuron, potassium current activated by action potential waveforms (inset) is completely inhibited by 0.2 mM 4-aminopyridine (which, in these cells, is probably selective for Kv3-mediated current). **c** | Effects on the firing of fast-spiking neocortical interneurons of 1 mM tetraethylammonium (TEA), which, in these neurons, appears to be selective for Kv3 channels. TEA produces broadening, a decreased rate of repolarization and a reduction in the afterhyperpolarization of spikes, along with slowing the firing frequency evoked by a constant current pulse, suggesting a major role for Kv3-mediated current in the firing of fast-spiking neocortical interneurons. **d** | Rescue of the fast-firing phenotype in oriens-alveus hippocampal interneurons by the addition of Kv3-like conductance with a dynamic clamp (BOX 2). 0.3 mM 4-aminopyridine slowed firing, but high-frequency firing was restored by the addition of artificial Kv3 conductance (rescue) by a dynamic clamp in the presence of 4-aminopyridine (giving ~95% restoration of action potential (AP) half-duration). Inst. AP freq., instantaneous AP frequency. Panel **a** modified, with permission, from REF. 31 © (2007) American Physiological Society. Panel **b** reproduced, with permission, from REF. 23 © (1998) Society for Neuroscience. Panel **c** reproduced, with permission, from REF. 6 © (1999) American Physiological Society. Panel **d** reproduced, with permission, from REF. 26 (2003) Society for Neuroscience.

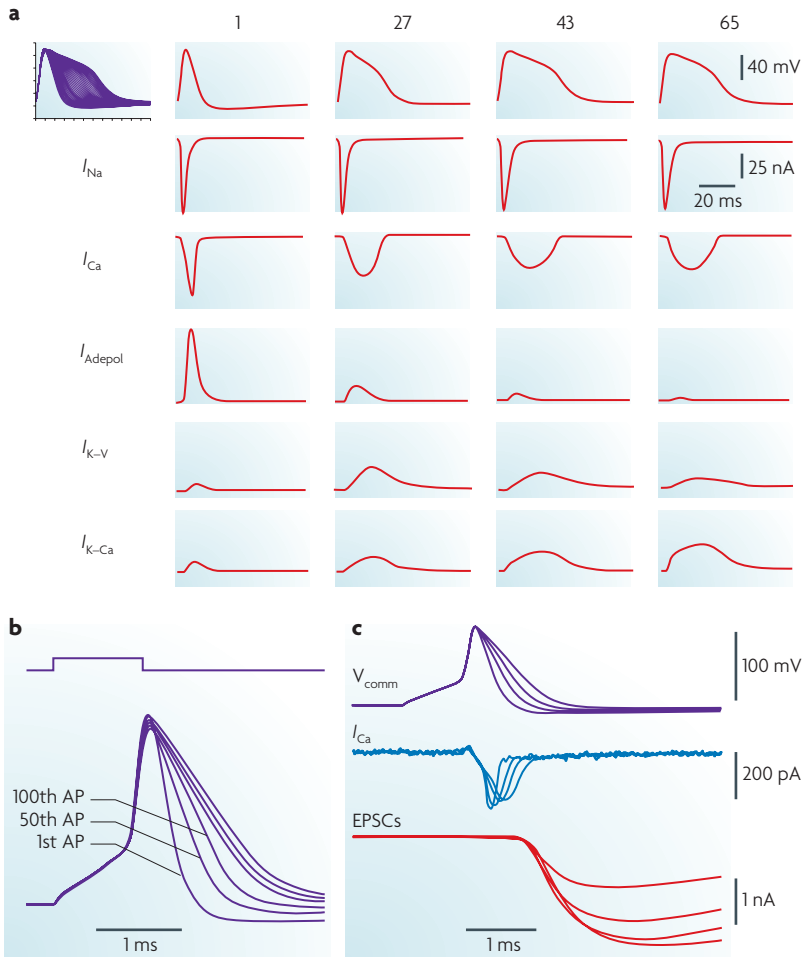

Figure 5 | **Frequency-dependent spike broadening from inactivation of potassium current. a** | Changes in currents accompanying frequency-dependent spike broadening in neuron R20 of *Aplysia*. A train of action potentials (first row) was evoked by stimulation at 7 Hz. Five major ionic currents were isolated by action potential clamp. Subtraction of currents before and after successive application of 60 μM tetrodotoxin, 3 mM tetraethylammonium (TEA), 40 mM TEA, 1 mM 4-aminopyridine, and 2 mM $CdCl_2$ was used to define I_{Na}, $I_{K–Ca}$ (calcium-activated K^+ current), $I_{K–V}$ (delayed-rectifier K^+ current), I_{Adepol} (I_A K^+ current), and I_{Ca}, respectively. Currents during the first spike, 27th spike (at which point $I_{K–V}$ reached its peak), 43rd spike (at which point the maximum broadening was reached) and last spike (65th) are shown. **b** | Frequency-dependent broadening of action potentials in mossy fibre boutons in the hippocampus. Every fiftieth action potential is shown, superimposed with the first. **c** | Potentiation of transmitter release at mossy fibre boutons by spike broadening. The waveforms recorded in panel **b** were applied as command waveforms (V_{comm}, top) in a voltage clamp to a different mossy fibre bouton, while both presynaptic calcium currents (middle) and excitatory postsynaptic currents (EPSCs, bottom) were recorded. Waveforms of action potentials 1, 25, 50 and 100 in the 50 Hz train were applied. The largest EPSC corresponds to the broadest presynaptic spike. Panel **a** reproduced, with permission, from REF. 135 © (1996) Society for Neuroscience. Panels **b**,**c** reproduced, with permission, from REF. 39 © (2000) Elsevier Science.

An elegant analysis of the mechanism of frequency-dependent broadening in this neuron[135] (FIG. 5a) provides an instructive example of how the techniques of action potential clamp and dynamic clamp (BOX 2) can be combined with conventional voltage clamp to experimentally attack a problem that otherwise might be approached purely through computer modelling. Action potential clamp showed that the current that changed most during frequency-dependent broadening was an I_A current that normally provides most of the repolarizing drive[134]. Puzzlingly, however, complete block of I_A (either pharmacologically or by dynamic clamp) produced much less broadening of the spike than occurs during frequency-dependent broadening. This is because modest increases in spike width result in increased activation of two other potassium currents, the activation of which during the spike is normally minimal: a delayed-rectifier current and a calcium-activated potassium current. Dynamic clamp analysis showed that a crucial factor in the greater degree of broadening seen during frequency-dependent changes is gradual use-dependent inactivation of the delayed rectifier current. This analysis illustrates several key aspects of the interaction of multiple currents in forming the action potential: first, the effect of pharmacologically blocking a single current may cause the role of that current to be underestimated, since the role of other currents can be drastically enhanced as a result of relatively modest changes in spike shape. Second, the role of any ionic current depends crucially on the context of all the other voltage-activated (and calcium-activated) channels in the membrane, and multiple currents may undergo frequency-dependent changes.

Frequency-dependent broadening of the action potential is also prominent in some mammalian neurons[19,37,83,86]. In hippocampal CA1 pyramidal neurons[83] and pyramidal-like projection neurons in the lateral amygdala[86], progressive inactivation of BK channels helps to produce frequency-dependent spike broadening. Inactivation of Kv4-mediated I_A also contributes to spike broadening in cell bodies of pyramidal neurons[125]. A particularly dramatic example of frequency-dependent spike broadening occurs at mossy fibre boutons in the hippocampus; this is probably mediated by inactivation of Kv1 family channels[39] (FIG. 5b) and is associated with pronounced synaptic facilitation (FIG. 5c).

Prelude to the spike: subthreshold currents

The ability of central neuron cell bodies to encode firing over a wide frequency range depends on multiple small currents flowing at subthreshold voltages, which speed or retard the approach to threshold and thereby influence the spike rate and pattern of firing. Subthreshold currents common in central neurons include I_A and I_D potassium currents, steady-state 'persistent' sodium currents, the current known as 'I_h' carried by hyperpolarization-activated cyclic nucleotide-gated (HCN) channels, and the current mediated by T-type (low-voltage-activated) calcium channels. Classic papers by Connor and Stevens[136,137] described a potassium current in molluscan neurons that they named 'A-type' current (I_A), which both activates and inactivates at subthreshold voltages, and explained how it enables repetitive firing at low frequencies: during the relative hyperpolarization after a spike, some inactivation is removed, then as the membrane depolarizes (still at subthreshold voltages), I_A increasingly activates (retarding the approach to threshold) but eventually inactivates, allowing threshold to be reached. I_D produces a subthreshold current with a similar role, but inactivates more slowly[50,129]. In many neurons, Kv1-mediated currents (in some cases called I_D

Delayed-rectifier current
Depolarization-activated potassium current similar to that of the squid axon, with relatively slow activation and minimal (or very slow) inactivation.

by virtue of dendrotoxin-sensitivity, but not necessarily showing the inactivation of I_D as originally described) have a major influence in determining firing patterns by flowing at subthreshold voltages before and between spikes, although they are swamped by other currents during the spike itself[34,36,132,138,139].

Virtually all central neurons appear to have a steady-state inward sodium current, sensitive to TTX, that flows at voltages between about –65 mV and –40 mV [7,48,63,76,77,97,98,140–145]. This 'persistent' sodium current activates with a voltage-dependence (e-fold for 4–6 mV) that is as steep as the voltage dependence of activation of the transient sodium current, but with a midpoint (typically ~–55 mV) about 30 mV below that of transient sodium current. Although maximum steady-state sodium current is only a tiny fraction (typically 0.5–5%) of the maximum transient sodium current, the resulting current of 5–200 pA is very significant functionally at subthreshold voltages. It has been argued that steady-state current amounting to ~0.5% of transient current is a necessary consequence of the normal gating behaviour of conventional sodium channels[98] (although an apparent counter-example of transient sodium current with no detectable persistent current has recently been described[144]). In addition to a persistent sodium current originating from the same population of channels underlying the transient sodium current[64,98,146], some neurons also clearly have specialized sodium channels that give subthreshold sodium currents far larger than 0.5% of the transient sodium current[147,148]. The molecular basis of these channels is not known. By producing a regenerative depolarizing current in the voltage range between the resting potential and spike threshold, persistent sodium current has a major role in determining the frequency and pattern of firing of many neurons[3,7,77,97,140,142,143,145,149–153].

T-type or low-voltage-activated calcium currents, originating from Cav3 family gene products, are also active at subthreshold voltages. One major function of the T-type calcium current is to produce rebound bursting following hyperpolarization (such as that from prolonged inhibitory input), which removes resting inactivation of the channels[154,155]. However, smaller steady currents can flow through T-type channels at resting potentials even without dynamic hyperpolarization and can influence firing patterns[156].

Because some currents flowing during the spike (including the transient sodium current and I_A potassium current) are sensitive to inactivation by changes in subthreshold voltages, spike shape can be significantly affected by the preceding voltage trajectory[39,157–159]. Remarkably, the electrotonic length constant of some central axons is sufficiently long that changes in somatic resting potential can affect the voltage in axons and nerve terminals hundreds of micrometres away[160,161] and, in some cases, alter the shape of presynaptic action potentials[161].

A remarkably poorly understood aspect of neuronal cellular neurophysiology is the collection of non-voltage-dependent conductances that determine resting potential, the foundation on which voltage-dependent subthreshold and suprathreshold currents exert their effects. The resting potassium conductance of neurons (and all cells) appears to depend on two-pore domain family (KCNK) potassium channels[162–165]. However, most neurons have resting potentials that are considerably more depolarized than the potassium equilibrium potential. In some neurons, there is evidence for a basal, non-voltage-dependent permeability to sodium ions[51,109,166], but the molecular basis for this is unknown.

The CNS includes many neurons that fire spontaneously in the absence of synaptic input[3]. The subthreshold current most closely identified with this electrical pacemaking is I_h [167,168]. Although I_h clearly has a major role in driving pacemaking in some central neurons[10,53,97,169,170], in others it appears that a TTX-sensitive persistent sodium current flowing at voltages positive to –65 mV is the major element driving the membrane to threshold[7,32,48,51,98,109]. Midbrain dopamine neurons are an interesting exception, where pacemaking seems to be driven mainly by a subthreshold calcium current[54,171].

After the spike is over

In the squid axon, the action potential is followed by an afterhyperpolarization, produced by the voltage-dependent potassium conductance activated during the spike, which transiently hyperpolarizes the membrane and then deactivates slowly over about 10 ms. For action potentials in mammalian neurons, afterhyperpolarizations are common but by no means universal. Distinct fast, medium and slow afterhyperpolarizations can often be recognized (FIG. 6a). Potassium channels contributing to afterhyperpolarizations include BK channels, SK channels[84,172,173] and Kv7 channels that mediate the M-current[89,174,175]. Usually, any afterhyperpolarization mediated by BK channels is brief[85,117,176,177], whereas those mediated by SK channels can last for hundreds of microseconds to seconds[172], reflecting the slow decay of intracellular calcium. Many pyramidal neurons have a slow component of the afterhyperpolarization that lasts for seconds, is not mediated by SK channels and has a molecular basis which remains a mystery[172,178–181].

In many neurons, including many pyramidal neurons in the cortex and hippocampus, the opposite of an afterhyperpolarization, an afterdepolarization, occurs: the membrane potential is depolarized relative to the resting potential[37,39,76,182–184]. Sometimes the afterdepolarization appears simply as a slow phase of repolarization at the end of the spike (FIG. 1b), but in other cases the voltage trajectory following the action potential has a clear rising phase (FIG. 6a). If the afterdepolarization is large enough to reach threshold, the result is all-or-none burst firing (FIG. 6b,c). Ionic currents contributing to afterdepolarizations include persistent sodium currents[140,149], resurgent sodium currents[48,76,185], T-type calcium currents[185], R-type calcium currents[186] and currents generated by calcium-activated non-selective cation channels[187].

The dendritic tree may also make important contributions to the afterdepolarization[188–191]. A purely electrotonic (non-active) mechanism is possible, in which an action potential in the cell body depolarizes the dendritic membrane (which has a much larger surface area and capacitance) and, after the somatic spike has repolarized, charge

e-fold
Measure of steepness of voltage-dependent activation, associated with a description by the Boltzmann function; e-fold increase is a 2.72-fold increase.

Midpoint
Voltage at which activation is half-maximal.

Rebound bursting
Firing of a burst of action potentials when a hyperpolarizing influence (such as inhibitory postsynaptic potential) is terminated.

Electrotonic length constant
Measure of the distance over which a voltage change imposed at one point in a cable-like structure decays to 1/e (~37%).

Pacemaking neurons
Neurons that fire spontaneous action potentials in a regular, rhythmic manner.

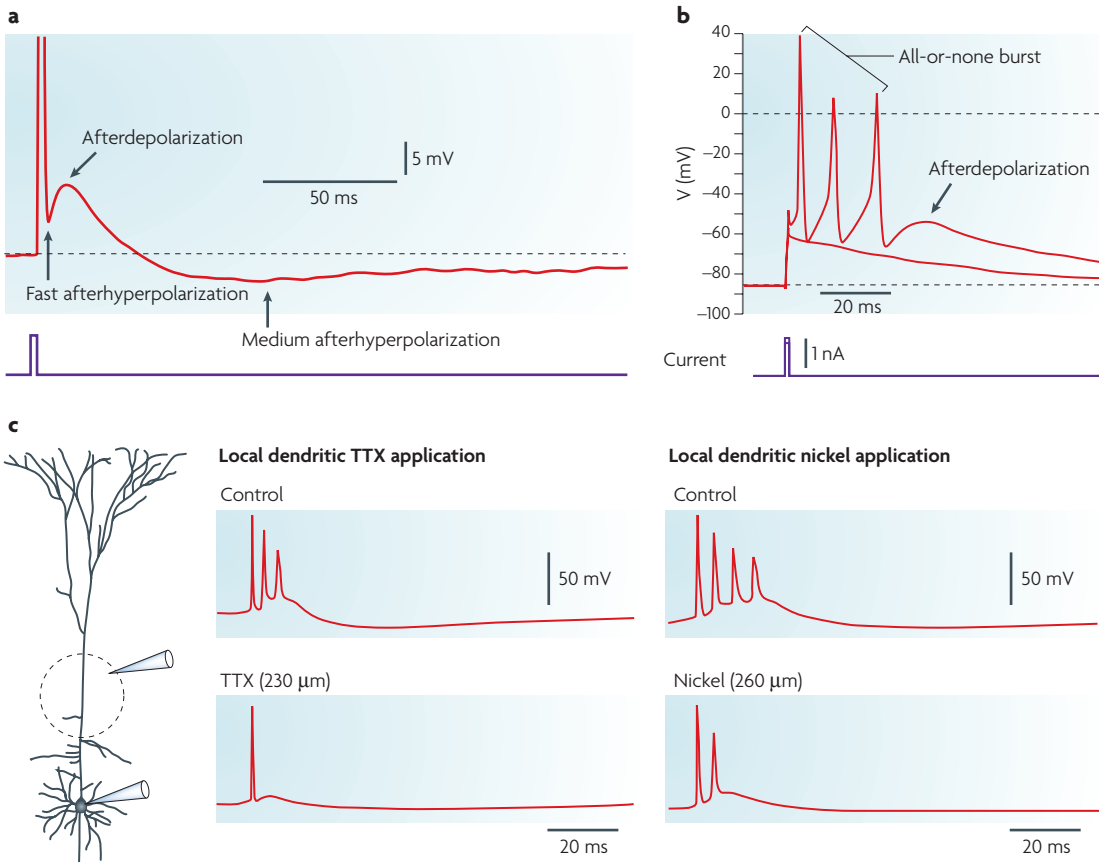

Figure 6 | **Afterhyperpolarizations, afterdepolarizations, and all-or-none burst firing. a** | Afterpotentials in a CA1 pyramidal neuron studied in brain slice. A slow afterhyperpolarization continues after the time shown, lasting more than a second (not shown). **b** | All-or-none burst firing resulting from afterdepolarizations in a dissociated cerebellar Purkinje neuron. The cell was held at –85 mV by a steady holding current of –40 pA (to stop spontaneous firing) and stimulated by brief (1 ms) current injections of 1.2 nA (which produced a subthreshold response) or 1.4 nA (which produced all-or-none burst firing). All-or-none burst firing results from afterdepolarizations that reach spike threshold. Arrow, afterdepolarization following the final spike in the burst. **c** | The contribution of dendritic sodium and calcium currents to burst firing in cortical layer 5 pyramidal neurons. Traces recorded at the soma show the effect in different cells of tetrodotoxin (TTX) (100 nM) or nickel (1 mM) applied locally to the apical dendrite 230–260 µm from the soma. Note that TTX did not change the amplitude, threshold or waveform of the first somatic action potential, verifying the confinement of TTX to the dendrite. The holding potential was –65 mV for both experiments. V, membrane voltage. Panel **a** reproduced, with permission, from REF. 117 © (1987) Cambridge Univ. Press. Panel **b** reproduced, with permission, from REF. 48 © (1997) Society for Neuroscience. Panel **c** reproduced, with permission, from REF. 191 © (1999) Cambridge Univ. Press.

from the depolarized dendritic membrane passes back to the soma and produces an afterdepolarization. This effect can be amplified by active dendritic conductances mediated by sodium and calcium channels[189–191] (FIG. 6c), which are commonly present in dendrites and produce large active depolarizing responses that are slower and occur later relative to the somatic action potential. However, even in the absence of contributions from dendritic depolarization, afterdepolarizations can be produced solely by ionic conductances in the cell body[140] and are prominent in acutely dissociated cell bodies from both pyramidal neurons[50] and Purkinje neurons[48,185].

Perspectives

Merely cataloguing all the components of ionic currents for any neuron is extremely challenging, as is characterizing the gating kinetics of any single component (as illustrated by the evolution of increasingly complex kinetic models for sodium channels, BOX 3). For currents such as I_A, I_D and TTX-sensitive sodium currents, the same channels can underlie both small subthreshold currents between spikes and large currents during the spike, producing highly complex gating behaviour as channels activate and inactivate on slow and fast timescales and influence both the approach to the spike and the spike itself. Accurately describing channel gating on both fast and slow timescales is difficult. However, the far greater challenge is to understand how all the voltage-dependent currents interact — with each conductance element both controlled by voltage and causing voltage to change — to control the generation of action potentials. Because of the two-way interactions between any pair of conductances, mediated by changes in membrane voltage on a sub-millisecond timescale, the role of any particular

Box 3 | **Limitations of the Hodgkin–Huxley model for channel kinetics**

The Hodgkin–Huxley explanation of the action potential — regenerative depolarization due to a steeply voltage-dependent sodium-selective conductance followed by repolarization due to inactivation of this conductance along with activation of a slower potassium conductance[1] — has been confirmed beyond doubt. In devising a mathematical model to predict the shape and propagation of the axon potential from their voltage-clamp data, Hodgkin and Huxley invented ingeniously simple mathematical expressions to account for the complex time- and voltage-dependent changes in sodium and potassium conductances. The simplicity of these expressions facilitated the tedious process of numerical integration. However, the Hodgkin–Huxley model of sodium current gating kinetics has subsequently been found to be at odds with the actual behaviour of sodium channels. In this model, the inactivation of channels is governed by a separate voltage-dependent process than that governing the activation of channels. In fact, various experiments have shown that inactivation derives its voltage-dependence from the same voltage-dependent steps as activation[2,66,67,201–203]. In modern models for sodium channel gating, inactivation is viewed as an inherently non-voltage-dependent process that is promoted by activation because activated channels can more readily undergo inactivation than non-activated channels[51,98,203,204]. The revised view of channel gating is most significant for predictions of the relative speed and completeness of activation and inactivation at subthreshold voltages — key for accurate predictions of repetitive firing — because the time-dependence and voltage-dependence of activation and inactivation are inherently intertwined. The same principles probably apply to other inactivating channels, such as T-type calcium channels and A-type potassium channels, and similar Markov models based on an allosteric relationship between activation and inactivation have been formulated to capture the kinetics of these channels[205,206]. However, kinetic models based on these advances in understanding channel gating are only beginning to be used in models of action potentials and firing patterns[46,76,146].

ionic conductance in influencing the action potential shape and firing pattern of a neuron depends crucially on what other ionic conductances are also present, and the effects of adding or deleting a given conductance can be counter-intuitive[6,135,145]. Although each neuronal type is different, there are undoubtedly general principles involving interactions among particular conductances waiting to be discovered.

Despite its complexity, the system of ionic currents in a neuron has remarkable advantages as a problem in 'systems biology', including highly quantifiable elements, highly quantifiable outputs (not just action potential shape but also firing rates and patterns) and a dynamic feedback mechanism based on a primary central quantity (membrane voltage) that can be measured extremely accurately. Because of these features, the system is ideally suited for mathematical modelling, probably more so than any other biological system, and relatively detailed models (including at least approximate kinetic descriptions of up to 11 different voltage-dependent conductances) have been formulated for the best-studied mammalian neurons[76,80,83,140,143,145,146,192,193]. Already, such modelling has given insight into an important general question in systems biology — how tolerant is the overall behaviour of the system to alterations in the magnitude or properties of system elements? In the case of burst firing of a particular neuron in the crab stomatogastric ganglion, electrophysiological experimentation and modelling have been combined to yield a remarkable finding: individual neurons with very similar firing properties can have densities of individual currents that vary several-fold[194–196], even though modest changes of a single conductance are capable of altering the firing of any given cell. Similar findings have been reported for the firing of cerebellar Purkinje neurons[193,197]. Related questions in a broad array of neurons with widely different functions in information processing can be attacked with an increasing array of powerful experimental tools. Knockout mouse models, RNA interference and new pharmacological agents allow the increasingly accurate definition of individual conductances, while the action potential clamp technique provides a direct, purely experimental integration between current clamp behaviour and voltage-clamp measurements. Such experimental advances will facilitate increasing detail and realism of computer models, with the dynamic clamp technique providing an especially powerful link between model and experiment.

1. Hodgkin, A. L. & Huxley, A. F. A quantitative description of membrane current and its application to conduction and excitation in nerve. *J. Physiol.* **117**, 500–544 (1952).
2. Hille, B. *Ion Channels of Excitable Membranes* (Sinauer, Sunderland, 2001).
3. Llinás, R. R. The intrinsic electrophysiological properties of mammalian neurons: insights into central nervous system function. *Science* **242**, 1654–1664 (1988).
Seminal review/manifesto by a pioneer of CNS cellular electrophysiology, surveying the wide variety of intrinsic excitability of central neurons and emphasizing the intrinsic oscillatory behaviour of cells and circuits.
4. Guttman, R. & Barnhill, R. Oscillation and repetitive firing in squid axons. Comparison of experiments with computations. *J. Gen. Physiol.* **55**, 104–118 (1970).
5. Connors, B. W. & Gutnick, M. J. Intrinsic firing patterns of diverse neocortical neurons. *Trends Neurosci.* **13**, 99–104 (1990).
6. Erisir, A., Lau, D., Rudy, B. & Leonard, C. S. Function of specific K^+ channels in sustained high-frequency firing of fast-spiking neocortical interneurons. *J. Neurophysiol.* **82**, 2476–2489 (1999).
7. Bevan, M. D. & Wilson, C. J. Mechanisms underlying spontaneous oscillation and rhythmic firing in rat subthalamic neurons. *J. Neurosci.* **19**, 7617–7628 (1999).
8. Nowak, L. G., Azouz, R., Sanchez-Vives, M. V., Gray, C. M. & McCormick, D. A. Electrophysiological classes of cat primary visual cortical neurons *in vivo* as revealed by quantitative analyses. *J. Neurophysiol.* **89**, 1541–1566 (2003).
9. Tateno, T., Harsch, A. & Robinson, H. P. Threshold firing frequency-current relationships of neurons in rat somatosensory cortex: type 1 and type 2 dynamics. *J. Neurophysiol.* **92**, 2283–2294 (2004).
10. Forti, L., Cesana, E., Mapelli, J. & D'Angelo, E. Ionic mechanisms of autorhythmic firing in rat cerebellar Golgi cells. *J. Physiol.* **574**, 711–729 (2006).
11. Hodgkin, A. L. The local electric changes associated with repetitive action in a non-medullated axon. *J. Physiol.* **107**, 165–181 (1948).
12. Connor, J. A. Neural repetitive firing: a comparative study of membrane properties of crustacean walking leg axons. *J. Neurophysiol.* **38**, 922–332 (1975).
13. Debanne, D. Information processing in the axon. *Nature Rev. Neurosci.* **5**, 304–316 (2004).
14. Coetzee, W. A. *et al.* Molecular diversity of K^+ channels. *Ann. NY Acad. Sci.* **868**, 233–285 (1999).
15. McCormick, D. A., Connors, B. W., Lighthall, J. W. & Prince, D. A. Comparative electrophysiology of pyramidal and sparsely spiny stellate neurons of the neocortex. *J. Neurophysiol.* **54**, 782–806 (1985).
Introduces 'regular-spiking', 'bursting' and 'fast-spiking' classifications of firing patterns of neocortical neurons, correlates firing patterns with spike shape, and identifies fast-spiking neocortical neurons as GABA-mediated interneurons.
16. Kawaguchi, Y. Physiological subgroups of nonpyramidal cells with specific morphological characteristics in layer II/III of rat frontal cortex. *J. Neurosci.* **15**, 2638–2655 (1995).
17. Mountcastle, V. B., Talbot, W. H., Sakata, H. & Hyvarinen, J. Cortical neuronal mechanisms in flutter-vibration studied in unanesthetized monkeys. Neuronal periodicity and frequency discrimination. *J. Neurophysiol.* **32**, 452–484 (1969).
18. Kawaguchi, Y. Physiological, morphological, and histochemical characterization of three classes of interneurons in rat neostriatum. *J. Neurosci.* **13**, 4908–4923 (1993).
19. Zhou, F. M. & Hablitz, J. J. Layer I neurons of rat neocortex. I. Action potential and repetitive firing properties. *J. Neurophysiol.* **76**, 651–667 (1996).
20. Descalzo, V. F., Nowak, L. G., Brumberg, J. C., McCormick, D. A. & Sanchez-Vives, M. V. Slow adaptation in fast-spiking neurons of visual cortex. *J. Neurophysiol.* **93**, 1111–1118 (2005).
21. Du, J., Zhang, L., Weiser, M., Rudy, B. & McBain, C. J. Developmental expression and functional characterization of the potassium-channel subunit Kv3.1b in parvalbumin-containing interneurons of the rat hippocampus. *J. Neurosci.* **16**, 506–518 (1996).
22. Massengill, J. L., Smith, M. A., Son, D. I. & O'Dowd, D. K. Differential expression of K4-AP currents and Kv3.1 potassium channel transcripts in cortical neurons that develop distinct firing phenotypes. *J. Neurosci.* **17**, 3136–3147 (1997).
23. Martina, M., Schultz, J. H., Ehmke, H., Monyer, H. & Jonas, P. Functional and molecular differences between voltage-gated K^+ channels of fast-spiking interneurons and pyramidal neurons of rat hippocampus. *J. Neurosci.* **18**, 8111–8125 (1998).

24. Lien, C. C., Martina, M., Schultz, J. H., Ehmke, H. & Jonas, P. Gating, modulation and subunit composition of voltage-gated K^+ channels in dendritic inhibitory interneurones of rat hippocampus. *J. Physiol.* **538**, 405–419 (2002).
25. Baranauskas, G., Tkatch, T., Nagata, K., Yeh, J. Z. & Surmeier, D. J. Kv3.4 subunits enhance the repolarizing efficiency of Kv3.1 channels in fast-spiking neurons. *Nature Neurosci.* **6**, 258–266 (2003).
26. Lien, C. C. & Jonas, P. Kv3 potassium conductance is necessary and kinetically optimized for high-frequency action potential generation in hippocampal interneurons. *J. Neurosci.* **23**, 2058–2068 (2003).
Uses the dynamic clamp technique to demonstrate that the Kv3-mediated potassium current speeds up firing and that deactivation kinetics are a crucial parameter for this effect.
27. Rudy, B. & McBain, C. J. Kv3 channels: voltage-gated K^+ channels designed for high-frequency repetitive firing. *Trends Neurosci.* **24**, 517–526 (2001).
Comprehensive review of the correlation between the expression of Kv3 channels and the fast-spiking phenotype.
28. Southan, A. P. & Robertson, B. Electrophysiological characterization of voltage-gated K^+ currents in cerebellar basket and purkinje cells: Kv1 and Kv3 channel subfamilies are present in basket cell nerve terminals. *J. Neurosci.* **20**, 114–122 (2000).
29. Martina, M., Yao, G. L. & Bean, B. P. Properties and functional role of voltage-dependent potassium channels in dendrites of rat cerebellar Purkinje neurons. *J. Neurosci.* **23**, 5698–5707 (2003).
30. McKay, B. E. & Turner, R. W. Kv3 K^+ channels enable burst output in rat cerebellar Purkinje cells. *Eur. J. Neurosci.* **20**, 729–739 (2004).
31. Martina, M., Metz, A. E. & Bean, B. P. Voltage-dependent potassium currents during fast spikes of rat cerebellar Purkinje neurons: inhibition by BDS-I toxin. *J. Neurophysiol.* **97**, 563–571 (2007).
32. Do, M. T. & Bean, B. P. Subthreshold sodium currents and pacemaking of subthalamic neurons: modulation by slow inactivation. *Neuron* **39**, 109–120 (2003).
33. Wigmore, M. A. & Lacey, M. G. A Kv3-like persistent, outwardly rectifying, Cs^+-permeable, K^+ current in rat subthalamic nucleus neurones. *J. Physiol.* **527**, 493–506 (2000).
34. Brew, H. M. & Forsythe, I. D. Two voltage-dependent K^+ conductances with complementary functions in postsynaptic integration at a central auditory synapse. *J. Neurosci.* **15**, 8011–8022 (1995).
35. Wang, L. Y., Gan, L., Forsythe, I. D. & Kaczmarek, L. K. Contribution of the Kv3.1 potassium channel to high-frequency firing in mouse auditory neurones. *J. Physiol.* **509**, 183–194 (1998).
36. Ishikawa, T. *et al.* Distinct roles of Kv1 and Kv3 potassium channels at the calyx of Held presynaptic terminal. *J. Neurosci.* **23**, 10445–10453 (2003).
37. Connors, B. W., Gutnick, M. J. & Prince, D. A. Electrophysiological properties of neocortical neurons *in vitro*. *J. Neurophysiol.* **48**, 1302–1320 (1982).
Classic description of all-or-none bursting, and of afterdepolarizations and action potential broadening, in neocortical pyramidal neurons.
38. Staff, N. P., Jung, H. Y., Thiagarajan, T., Yao, M. & Spruston, N. Resting and active properties of pyramidal neurons in subiculum and CA1 of rat hippocampus. *J. Neurophysiol.* **84**, 2398–2408 (2000).
39. Geiger, J. R. & Jonas, P. Dynamic control of presynaptic Ca^{2+} inflow by fast-inactivating K^+ channels in hippocampal mossy fiber boutons. *Neuron* **28**, 927–939 (2000).
Remarkable sequence of current-clamp and voltage-clamp recordings from presynaptic terminals of mossy fibres and their postsynaptic targets, showing that presynaptic spikes are narrower than those in the cell body, that presynaptic spikes undergo frequency-dependent broadening due to inactivation of Kv1 family channels, and that spike broadening produces dramatic synaptic facilitation.
40. Coombs, J. S., Curtis, D. R. & Eccles, J. C. The interpretation of spike potentials of motoneurones. *J. Physiol.* **139**, 198–231 (1957).
41. Grace, A. A. & Bunney, B. S. Intracellular and extracellular electrophysiology of nigral dopaminergic neurons—2. Action potential generating mechanisms and morphological correlates. *Neuroscience* **10**, 317–331 (1983).
42. Hausser, M., Stuart, G., Racca, C. & Sakmann, B. Axonal initiation and active dendritic propagation of action potentials in substantia nigra neurons. *Neuron* **15**, 637–647 (1995).
43. Stuart, G., Schiller, J. & Sakmann, B. Action potential initiation and propagation in rat neocortical pyramidal neurons. *J. Physiol.* **505**, 617–632 (1997).
Uses double (and triple) patch pipette recordings in layer 5 pyramidal neurons to directly demonstrate that spikes are initiated in the axon before the soma — even with strong synaptic stimulation that first elicits regenerative potentials in dendrites. Also demonstrates back-propagation of axonal spikes into the dendritic tree.
44. Martina, M., Vida, I. & Jonas, P. Distal initiation and active propagation of action potentials in interneuron dendrites. *Science* **287**, 295–300 (2000).
45. Palmer, L. M. & Stuart, G. J. Site of action potential initiation in layer 5 pyramidal neurons. *J. Neurosci.* **26**, 1854–1863 (2006).
46. Khaliq, Z. M. & Raman, I. M. Relative contributions of axonal and somatic Na channels to action potential initiation in cerebellar Purkinje neurons. *J. Neurosci.* **26**, 1935–1944 (2006).
47. Shu, Y., Duque, A., Yu, Y., Haider, B. & McCormick, D. A. Properties of action-potential initiation in neocortical pyramidal cells: evidence from whole cell axon recordings. *J. Neurophysiol.* **97**, 746–760 (2007).
48. Raman, I. M. & Bean, B. P. Resurgent sodium current and action potential formation in dissociated cerebellar Purkinje neurons. *J. Neurosci.* **17**, 4517–4526 (1997).
49. Kay, A. R. & Wong, R. K. Isolation of neurons suitable for patch-clamping from adult mammalian central nervous systems. *J. Neurosci. Methods* **16**, 227–238 (1986).
50. Mitterdorfer, J. & Bean, B. P. Potassium currents during the action potential of hippocampal CA3 neurons. *J. Neurosci.* **22**, 10106–10115 (2002).
51. Raman, I. M., Gustafson, A. E. & Padgett, D. Ionic currents and spontaneous firing in neurons isolated from the cerebellar nuclei. *J. Neurosci.* **20**, 9004–9016 (2000).
52. Shen, W., Hernandez-Lopez, S., Tkatch, T., Held, J. E. & Surmeier, D. J. Kv1.2-containing K^+ channels regulate subthreshold excitability of striatal medium spiny neurons. *J. Neurophysiol.* **91**, 1337–1349 (2004).
53. Chan, C. S., Shigemoto, R., Mercer, J. N. & Surmeier, D. J. HCN2 and HCN1 channels govern the regularity of autonomous pacemaking and synaptic resetting in globus pallidus neurons. *J. Neurosci.* **24**, 9921–9932 (2004).
54. Puopolo, M., Raviola, E. & Bean, B. P. Roles of subthreshold calcium current and sodium current in spontaneous firing of mouse midbrain dopamine neurons. *J. Neurosci.* **27**, 645–656 (2007).
55. Nam, S. C. & Hockberger, P. E. Analysis of spontaneous electrical activity in cerebellar Purkinje cells acutely isolated from postnatal rats. *J. Neurobiol.* **33**, 18–32 (1997).
56. Callaway, J. C. & Ross, W. N. Spatial distribution of synaptically activated sodium concentration changes in cerebellar Purkinje neurons. *J. Neurophysiol.* **77**, 145–152 (1997).
57. Hausser, M. & Clark, B. A. Tonic synaptic inhibition modulates neuronal output pattern and spatiotemporal synaptic integration. *Neuron* **19**, 665–678 (1997).
58. Jenerick, H. Phase plane trajectories of the muscle spike potential. *Biophys. J.* **3**, 363–377 (1963).
59. Hodgkin, A. L., Huxley, A. F. & Katz, B. Measurement of current-voltage relations in the membrane of the giant axon of *Loligo*. *J. Physiol.* **116**, 424–448 (1952).
60. Colbert, C. M. & Johnston, D. Axonal action-potential initiation and Na^+ channel densities in the soma and axon initial segment of subicular pyramidal neurons. *J. Neurosci.* **16**, 6676–6686 (1996).
61. Clark, B. A., Monsivais, P., Branco, T., London, M. & Hausser, M. The site of action potential initiation in cerebellar Purkinje neurons. *Nature Neurosci.* **8**, 137–139 (2005).
62. Martina, M. & Jonas, P. Functional differences in Na^+ channel gating between fast-spiking interneurones and principal neurones of rat hippocampus. *J. Physiol.* **505**, 593–603 (1997).
63. Maurice, N., Tkatch, T., Meisler, M., Sprunger, L. K. & Surmeier, D. J. D1/D5 dopamine receptor activation differentially modulates rapidly inactivating and persistent sodium currents in prefrontal cortex pyramidal neurons. *J. Neurosci.* **21**, 2268–2277 (2001).
64. Ptak, K. *et al.* Sodium currents in medullary neurons isolated from the pre-Botzinger complex region. *J. Neurosci.* **25**, 5159–5170 (2005).
65. Baranauskas, G. & Martina, M. Sodium currents activate without a Hodgkin-and-Huxley-type delay in central mammalian neurons. *J. Neurosci.* **26**, 671–684 (2006).
66. Armstrong, C. M. & Bezanilla, F. Inactivation of the sodium channel. II. Gating current experiments. *J. Gen. Physiol.* **70**, 567–590 (1977).
67. Bezanilla, F. & Armstrong, C. M. Inactivation of the sodium channel. I. Sodium current experiments. *J. Gen. Physiol.* **70**, 549–566 (1977).
68. Engel, D. & Jonas, P. Presynaptic action potential amplification by voltage-gated Na^+ channels in hippocampal mossy fiber boutons. *Neuron* **45**, 405–417 (2005).
69. Neumcke, B. & Stampfli, R. Sodium currents and sodium-current fluctuations in rat myelinated nerve fibres. *J. Physiol.* **329**, 163–184 (1982).
70. Neumcke, B., Schwarz, J. R. & Stampfli, R. A comparison of sodium currents in rat and frog myelinated nerve: normal and modified sodium inactivation. *J. Physiol.* **382**, 175–191 (1987).
71. Naundorf, B., Wolf, F. & Volgushev, M. Unique features of action potential initiation in cortical neurons. *Nature* **440**, 1060–1063 (2006).
72. McCormick, D. A., Shu, Y. & Yu, Y. Neurophysiology: Hodgkin and Huxley model — still standing? *Nature* **445**, E1—E2 (2007).
73. Raman, I. M. & Bean, B. P. Inactivation and recovery of sodium currents in cerebellar Purkinje neurons: evidence for two mechanisms. *Biophys. J.* **80**, 729–737 (2001).
74. Grieco, T. M., Malhotra, J. D., Chen, C., Isom, L. L. & Raman, I. M. Open-channel block by the cytoplasmic tail of sodium channel β4 as a mechanism for resurgent sodium current. *Neuron* **45**, 233–244 (2005).
Presents evidence for a likely molecular mechanism underlying resurgent sodium currents.
75. Afshari, F. S. *et al.* Resurgent Na currents in four classes of neurons of the cerebellum. *J. Neurophysiol.* **92**, 2831–2843 (2004).
76. Magistretti, J., Castelli, L., Forti, L. & D'Angelo, E. Kinetic and functional analysis of transient, persistent and resurgent sodium currents in rat cerebellar granule cells *in situ*: an electrophysiological and modelling study. *J. Physiol.* **573**, 83–106 (2006).
State-of-the-art combination of voltage-clamp analysis of currents and modelling of firing, using a model with nine distinct conductances including an allosteric sodium channel model.
77. Enomoto, A., Han, J. M., Hsiao, C. F., Wu, N. & Chandler, S. H. Participation of sodium currents in burst generation and control of membrane excitability in mesencephalic trigeminal neurons. *J. Neurosci.* **26**, 3412–3422 (2006).
78. Leao, R. N., Naves, M. M., Leao, K. E. & Walmsley, B. Altered sodium currents in auditory neurons of congenitally deaf mice. *Eur. J. Neurosci.* **24**, 1137–1146 (2006).
79. Cummins, T. R., Dib-Hajj, S. D., Herzog, R. I. & Waxman, S. G. Nav1.6 channels generate resurgent sodium currents in spinal sensory neurons. *FEBS Lett.* **579**, 2166–2170 (2005).
80. Khaliq, Z. M., Gouwens, N. W. & Raman, I. M. The contribution of resurgent sodium current to high-frequency firing in Purkinje neurons: an experimental and modeling study. *J. Neurosci.* **23**, 4899–4912 (2003).
81. Sah, P. & McLachlan, E. M. Potassium currents contributing to action potential repolarization and the afterhyperpolarization in rat vagal motoneurons. *J. Neurophysiol.* **68**, 1834–1841 (1992).
82. Sah, P. Ca^{2+}-activated K^+ currents in neurones: types, physiological roles and modulation. *Trends Neurosci.* **19**, 150–154 (1996).
83. Shao, L. R., Halvorsrud, R., Borg-Graham, L. & Storm, J. F. The role of BK-type Ca^{2+}-dependent K^+ channels in spike broadening during repetitive firing in rat hippocampal pyramidal cells. *J. Physiol.* **521**, 135–146 (1999).
84. Sah, P. & Faber, E. S. Channels underlying neuronal calcium-activated potassium currents. *Prog. Neurobiol.* **66**, 345–353 (2002).
85. Faber, E. S. & Sah, P. Physiological role of calcium-activated potassium currents in the rat lateral amygdala. *J. Neurosci.* **22**, 1618–1628 (2002).
86. Faber, E. S. & Sah, P. Ca^{2+}-activated K^+ (BK) channel inactivation contributes to spike broadening during repetitive firing in the rat lateral amygdala. *J. Physiol.* **552**, 483–497 (2003).

87. Sun, X., Gu, X. Q. & Haddad, G. G. Calcium influx via L- and N-type calcium channels activates a transient large-conductance Ca^{2+}-activated K^+ current in mouse neocortical pyramidal neurons. *J. Neurosci.* **23**, 3639–3648 (2003).
88. Goldberg, J. A. & Wilson, C. J. Control of spontaneous firing patterns by the selective coupling of calcium currents to calcium-activated potassium currents in striatal cholinergic interneurons. *J. Neurosci.* **25**, 10230–10238 (2005).
89. Storm, J. F. Potassium currents in hippocampal pyramidal cells. *Prog. Brain Res.* **83**, 161–187 (1990).
90. Chen, W., Zhang, J. J., Hu, G. Y. & Wu, C. P. Different mechanisms underlying the repolarization of narrow and wide action potentials in pyramidal cells and interneurons of cat motor cortex. *Neuroscience* **73**, 57–68 (1996).
91. Lancaster, B. & Nicoll, R. A. Properties of two calcium-activated hyperpolarizations in rat hippocampal neurones. *J. Physiol.* **389**, 187–203 (1987).
92. Storm, J. F. Intracellular injection of a Ca^{2+} chelator inhibits spike repolarization in hippocampal neurons. *Brain Res.* **435**, 387–392 (1987).
93. Marrion, N. V. & Tavalin, S. J. Selective activation of Ca^{2+}-activated K^+ channels by co-localized Ca^{2+} channels in hippocampal neurons. *Nature* **395**, 900–905 (1998).
94. Grunnet, M. & Kaufmann, W. A. Coassembly of big conductance Ca^{2+}-activated K^+ channels and L-type voltage-gated Ca^{2+} channels in rat brain. *J. Biol. Chem.* **279**, 36445–36453 (2004).
95. Berkefeld, H. *et al.* BK_{Ca}-Cav channel complexes mediate rapid and localized Ca^{2+}-activated K^+ signaling. *Science* **314**, 615–620 (2006).
96. Muller, A., Kukley, M., Uebachs, M., Beck, H. & Dietrich, D. Nanodomains of single Ca^{2+} channels contribute to action potential repolarization in cortical neurons. *J. Neurosci.* **27**, 483–495 (2007).
97. Bennett, B. D., Callaway, J. C. & Wilson, C. J. Intrinsic membrane properties underlying spontaneous tonic firing in neostriatal cholinergic interneurons. *J. Neurosci.* **20**, 8493–8503 (2000).
A combination of current-clamp, voltage-clamp and calcium imaging to determine the ionic mechanism of pacemaking in tonically active cholinergic neurons of the striatum.
98. Taddese, A. & Bean, B. P. Subthreshold sodium current from rapidly inactivating sodium channels drives spontaneous firing of tuberomammillary neurons. *Neuron* **33**, 587–600 (2002).
99. Viana, F., Bayliss, D. A. & Berger, A. J. Multiple potassium conductances and their role in action potential repolarization and repetitive firing behavior of neonatal rat hypoglossal motoneurons. *J. Neurophysiol.* **69**, 2150–2163 (1993).
100. Williams, S., Serafin, M., Muhlethaler, M. & Bernheim, L. Distinct contributions of high- and low-voltage-activated calcium currents to afterhyperpolarizations in cholinergic nucleus basalis neurons of the guinea pig. *J. Neurosci.* **17**, 7307–7315 (1997).
101. Pineda, J. C., Waters, R. S. & Foehring, R. C. Specificity in the interaction of HVA Ca^{2+} channel types with Ca^{2+}-dependent AHPs and firing behavior in neocortical pyramidal neurons. *J. Neurophysiol.* **79**, 2522–2534 (1998).
102. Wolfart, J. & Roeper, J. Selective coupling of T-type calcium channels to SK potassium channels prevents intrinsic bursting in dopaminergic midbrain neurons. *J. Neurosci.* **22**, 3404–3413 (2002).
103. Hallworth, N. E., Wilson, C. J. & Bevan, M. D. Apamin-sensitive small conductance calcium-activated potassium channels, through their selective coupling to voltage-gated calcium channels, are critical determinants of the precision, pace, and pattern of action potential generation in rat subthalamic nucleus neurons *in vitro*. *J. Neurosci.* **23**, 7525–7542 (2003).
104. Womack, M. D., Chevez, C. & Khodakhah, K. Calcium-activated potassium channels are selectively coupled to P/Q-type calcium channels in cerebellar Purkinje neurons. *J. Neurosci.* **24**, 8818–8822 (2004).
105. Nedergaard, S. A Ca^{2+}-independent slow afterhyperpolarization in substantia nigra compacta neurons. *Neuroscience* **125**, 841–852 (2004).
106. Wolfart, J., Neuhoff, H., Franz, O. & Roeper, J. Differential expression of the small-conductance, calcium-activated potassium channel SK3 is critical for pacemaker control in dopaminergic midbrain neurons. *J. Neurosci.* **21**, 3443–3456 (2001).
107. Walter, J. T., Alvina, K., Womack, M. D., Chevez, C. & Khodakhah, K. Decreases in the precision of Purkinje cell pacemaking cause cerebellar dysfunction and ataxia. *Nature Neurosci.* **9**, 389–397 (2006).
108. Raman, I. M. & Bean, B. P. Ionic currents underlying spontaneous action potentials in isolated cerebellar Purkinje neurons. *J. Neurosci.* **19**, 1663–1674 (1999).
109. Jackson, A. C., Yao, G. L. & Bean, B. P. Mechanism of spontaneous firing in dorsomedial suprachiasmatic nucleus neurons. *J. Neurosci.* **24**, 7985–7998 (2004).
110. Llinās, R., Sugimori, M. & Simon, S. M. Transmission by presynaptic spike-like depolarization in the squid giant synapse. *Proc. Natl Acad. Sci. USA* **79**, 2415–2419 (1982).
111. Jackson, M. B., Konnerth, A. & Augustine, G. J. Action potential broadening and frequency-dependent facilitation of calcium signals in pituitary nerve terminals. *Proc. Natl Acad. Sci. USA* **88**, 380–384 (1991).
112. Borst, J. G. & Sakmann, B. Effect of changes in action potential shape on calcium currents and transmitter release in a calyx-type synapse of the rat auditory brainstem. *Philos. Trans. R. Soc. Lond. B Biol. Sci.* **354**, 347–355 (1999).
Action potential clamp experiments on presynaptic terminals (calyx of Held) showing that calcium channels are activated with high efficacy by action potentials.
113. Bischofberger, J., Geiger, J. R. & Jonas, P. Timing and efficacy of Ca^{2+} channel activation in hippocampal mossy fiber boutons. *J. Neurosci.* **22**, 10593–10602 (2002).
114. Yang, Y. M. & Wang, L. Y. Amplitude and kinetics of action potential-evoked Ca^{2+} current and its efficacy in triggering transmitter release at the developing calyx of held synapse. *J. Neurosci.* **26**, 5698–5708 (2006).
115. Fernandez, F. R., Mehaffey, W. H., Molineux, M. L. & Turner, R. W. High-threshold K^+ current increases gain by offsetting a frequency-dependent increase in low-threshold K^+ current. *J. Neurosci.* **25**, 363–371 (2005).
116. Akemann, W. & Knopfel, T. Interaction of Kv3 potassium channels and resurgent sodium current influences the rate of spontaneous firing of Purkinje neurons. *J. Neurosci.* **26**, 4602–4612 (2006).
117. Storm, J. F. Action potential repolarization and a fast after-hyperpolarization in rat hippocampal pyramidal cells. *J. Physiol.* **385**, 733–759 (1987).
Analysis using pharmacology and ionic substitution of the potassium currents underlying spike repolarization, fast, medium and slow afterhyperpolarizations in CA1 pyramidal neurons.
118. Locke, R. E. & Nerbonne, J. M. Three kinetically distinct Ca^{2+}-independent depolarization-activated K^+ currents in callosal-projecting rat visual cortical neurons. *J. Neurophysiol.* **78**, 2309–2320 (1997).
119. Locke, R. E. & Nerbonne, J. M. Role of voltage-gated K^+ currents in mediating the regular-spiking phenotype of callosal-projecting rat visual cortical neurons. *J. Neurophysiol.* **78**, 2321–2335 (1997).
120. Golding, N. L., Jung, H. Y., Mickus, T. & Spruston, N. Dendritic calcium spike initiation and repolarization are controlled by distinct potassium channel subtypes in CA1 pyramidal neurons. *J. Neurosci.* **19**, 8789–8798 (1999).
121. Kang, J., Huguenard, J. R. & Prince, D. A. Voltage-gated potassium channels activated during action potentials in layer V neocortical pyramidal neurons. *J. Neurophysiol.* **83**, 70–80 (2000).
122. Wu, R. L. & Barish, M. E. Two pharmacologically and kinetically distinct transient potassium currents in cultured embryonic mouse hippocampal neurons. *J. Neurosci.* **12**, 2235–2246 (1992).
123. Wu, R. L. & Barish, M. E. Modulation of a slowly inactivating potassium current, I_D, by metabotropic glutamate receptor activation in cultured hippocampal pyramidal neurons. *J. Neurosci.* **19**, 6825–6837 (1999).
124. Riazanski, V. *et al.* Functional and molecular analysis of transient voltage-dependent K^+ currents in rat hippocampal granule cells. *J. Physiol.* **537**, 391–406 (2001).
125. Kim, J., Wei, D. S. & Hoffman, D. A. Kv4 potassium channel subunits control action potential repolarization and frequency-dependent broadening in rat hippocampal CA1 pyramidal neurones. *J. Physiol.* **569**, 41–57 (2005).
126. Yuan, W., Burkhalter, A. & Nerbonne, J. M. Functional role of the fast transient outward K^+ current I_A in pyramidal neurons in (rat) primary visual cortex. *J. Neurosci.* **25**, 9185–9194 (2005).
127. Shibata, R. *et al.* A-type K^+ current mediated by the Kv4 channel regulates the generation of action potential in developing cerebellar granule cells. *J. Neurosci.* **20**, 4145–4155 (2000).
128. Sheng, M., Tsaur, M. L., Jan, Y. N. & Jan, L. Y. Subcellular segregation of two A-type K^+ channel proteins in rat central neurons. *Neuron* **9**, 271–284 (1992).
129. Storm, J. F. Temporal integration by a slowly inactivating K^+ current in hippocampal neurons. *Nature* **336**, 379–381 (1988).
Description of I_D as a subthreshold, slowly inactivating potassium current sensitive to low concentrations of 4-aminopyridine and distinct from I_A and delayed-rectifier potassium currents.
130. Stansfeld, C. E., Marsh, S. J., Halliwell, J. V. & Brown, D. A. 4-Aminopyridine and dendrotoxin induce repetitive firing in rat visceral sensory neurones by blocking a slowly inactivating outward current. *Neurosci. Lett.* **64**, 299–304 (1986).
131. Bekkers, J. M. & Delaney, A. J. Modulation of excitability by α-dendrotoxin-sensitive potassium channels in neocortical pyramidal neurons. *J. Neurosci.* **21**, 6553–6560 (2001).
132. Guan, D., Lee, J. C., Higgs, M. H., Spain, W. J. & Foehring, R. C. Functional roles of Kv1 channels in neocortical pyramidal neurons. *J. Neurophysiol.* **97**, 1931–1940 (2007).
133. Spain, W. J., Schwindt, P. C. & Crill, W. E. Two transient potassium currents in layer V pyramidal neurones from cat sensorimotor cortex. *J. Physiol.* **434**, 591–607 (1991).
134. Ma, M. & Koester, J. Consequences and mechanisms of spike broadening of R20 cells in *Aplysia californica*. *J. Neurosci.* **15**, 6720–6734 (1995).
135. Ma, M. & Koester, J. The role of K^+ currents in frequency-dependent spike broadening in *Aplysia* R20 neurons: a dynamic-clamp analysis. *J. Neurosci.* **16**, 4089–4101 (1996).
Combines the use of action potential clamp and dynamic clamp to analyse the changes in ionic currents underlying frequency-dependent spike broadening in an *Aplysia* neuron.
136. Connor, J. A. & Stevens, C. F. Voltage clamp studies of a transient outward membrane current in gastropod neural somata. *J. Physiol.* **213**, 21–30 (1971).
137. Connor, J. A. & Stevens, C. F. Prediction of repetitive firing behaviour from voltage clamp data on an isolated neurone soma. *J. Physiol.* **213**, 31–53 (1971).
Classic pair of papers describing I_A in a snail neuron and using a computer model to analyse how it enables steady low-frequency firing.
138. Dodson, P. D., Barker, M. C. & Forsythe, I. D. Two heteromeric Kv1 potassium channels differentially regulate action potential firing. *J. Neurosci.* **22**, 6953–6961 (2002).
139. McKay, B. E., Molineux, M. L., Mehaffey, W. H. & Turner, R. W. Kv1 K^+ channels control Purkinje cell output to facilitate postsynaptic rebound discharge in deep cerebellar neurons. *J. Neurosci.* **25**, 1481–1492 (2005).
140. Golomb, D., Yue, C. & Yaari, Y. Contribution of persistent Na^+ current and M-type K^+ current to somatic bursting in CA1 pyramidal cells: combined experimental and modeling study. *J. Neurophysiol.* **96**, 1912–1926 (2006).
141. Crill, W. E. Persistent sodium current in mammalian central neurons. *Annu. Rev. Physiol.* **58**, 349–362 (1996).
142. Brumberg, J. C., Nowak, L. G. & McCormick, D. A. Ionic mechanisms underlying repetitive high-frequency burst firing in supragranular cortical neurons. *J. Neurosci.* **20**, 4829–4843 (2000).
143. Hu, H., Vervaeke, K. & Storm, J. F. Two forms of electrical resonance at theta frequencies, generated by M-current, h-current and persistent Na^+ current in rat hippocampal pyramidal cells. *J. Physiol.* **545**, 783–805 (2002).
144. Astman, N., Gutnick, M. J. & Fleidervish, I. A. Persistent sodium current in layer 5 neocortical neurons is primarily generated in the proximal axon. *J. Neurosci.* **26**, 3465–3473 (2006).
145. Vervaeke, K., Hu, H., Graham, L. J. & Storm, J. F. Contrasting effects of the persistent Na^+ current on neuronal excitability and spike timing. *Neuron* **49**, 257–270 (2006).
Clear illustration of the context-sensitivity of the role of a given conductance, using dynamic clamp and an unusually detailed model of firing (incorporating 11 voltage-dependent conductances) to analyse counter-intuitive effects of a persistent sodium current on the firing patterns of CA1 pyramidal neurons.

146. Maurice, N. *et al.* D2 dopamine receptor-mediated modulation of voltage-dependent Na^+ channels reduces autonomous activity in striatal cholinergic interneurons. *J. Neurosci.* **24**, 10289–10301 (2004). **Combines current clamp, voltage clamp, and modelling to show that modest changes in sodium channel gating produced by dopamine can produce surprisingly large effects on the frequency of spontaneous firing.**
147. Magistretti, J. & Alonso, A. Biophysical properties and slow voltage-dependent inactivation of a sustained sodium current in entorhinal cortex layer-II principal neurons: a whole-cell and single-channel study. *J. Gen. Physiol.* **114**, 491–509 (1999).
148. Magistretti, J. & Alonso, A. Fine gating properties of channels responsible for persistent sodium current generation in entorhinal cortex neurons. *J. Gen. Physiol.* **120**, 855–873 (2002).
149. Azouz, R., Jensen, M. S. & Yaari, Y. Ionic basis of spike after-depolarization and burst generation in adult rat hippocampal CA1 pyramidal cells. *J. Physiol.* **492**, 211–223 (1996).
150. Gutfreund, Y., yarom, Y. & Segev, I. Subthreshold oscillations and resonant frequency in guinea-pig cortical neurons: physiology and modelling. *J. Physiol.* **483**, 621–640 (1995).
151. Hutcheon, B., Miura, R. M. & Puil, E. Subthreshold membrane resonance in neocortical neurons. *J. Neurophysiol.* **76**, 683–697 (1996).
152. White, J. A., Klink, R., Alonso, A. & Kay, A. R. Noise from voltage-gated ion channels may influence neuronal dynamics in the entorhinal cortex. *J. Neurophysiol.* **80**, 262–269 (1998).
153. Wu, N. *et al.* Persistent sodium currents in mesencephalic v neurons participate in burst generation and control of membrane excitability. *J. Neurophysiol.* **93**, 2710–2722 (2005).
154. Llinás, R. & Yarom, Y. Electrophysiology of mammalian inferior olivary neurones *in vitro*. Different types of voltage-dependent ionic conductances. *J. Physiol.* **315**, 549–567 (1981).
155. Jahnsen, H. & Llinás, R. Ionic basis for the electro-responsiveness and oscillatory properties of guinea-pig thalamic neurones *in vitro*. *J. Physiol.* **349**, 227–247 (1984).
156. Williams, S. R., Toth, T. I., Turner, J. P., Hughes, S. W. & Crunelli, V. The 'window' component of the low threshold Ca^{2+} current produces input signal amplification and bistability in cat and rat thalamocortical neurones. *J. Physiol.* **505**, 689–705 (1997).
157. Henze, D. A. & Buzsaki, G. Action potential threshold of hippocampal pyramidal cells *in vivo* is increased by recent spiking activity. *Neuroscience* **105**, 121–130 (2001).
158. de Polavieja, G. G., Harsch, A., Kleppe, I., Robinson, H. P. & Juusola, M. Stimulus history reliably shapes action potential waveforms of cortical neurons. *J. Neurosci.* **25**, 5657–5665 (2005).
159. Korngreen, A., Kaiser, K. M. & Zilberter, Y. Subthreshold inactivation of voltage-gated K^+ channels modulates action potentials in neocortical bitufted interneurones from rats. *J. Physiol.* **562**, 421–437 (2005).
160. Alle, H. & Geiger, J. R. Combined analog and action potential coding in hippocampal mossy fibers. *Science* **311**, 1290–1293 (2006).
161. Shu, Y., Hasenstaub, A., Duque, A., Yu, Y. & McCormick, D. A. Modulation of intracortical synaptic potentials by presynaptic somatic membrane potential. *Nature* **441**, 761–765 (2006). **References 160 and 161 demonstrate, in two types of glutamatergic neurons, that the electrotonic length constant of the axon is long enough (400–450 μm) that changes in membrane potential at the soma can influence membrane potential at presynaptic terminals.**
162. Goldstein, S. A., Bockenhauer, D., O'Kelly, I. & Zilberberg, N. Potassium leak channels and the KCNK family of two-P-domain subunits. *Nature Rev. Neurosci.* **2**, 175–184 (2001).
163. Meuth, S. G. *et al.* Membrane resting potential of thalamocortical relay neurons is shaped by the interaction among TASK3 and HCN2 channels. *J. Neurophysiol.* **96**, 1517–1529 (2006).
164. Mathie, A. Neuronal two-pore-domain potassium channels and their regulation by G protein-coupled receptors. *J. Physiol.* **578**, 377–385 (2007).
165. Berg, A. P. & Bayliss, D. A. Striatal cholinergic interneurons express a receptor-insensitive homomeric TASK-3-like background K^+ current. *J. Neurophysiol.* **97**, 1546–1552 (2007).
166. Eggermann, E. *et al.* The wake-promoting hypocretin-orexin neurons are in an intrinsic state of membrane depolarization. *J. Neurosci.* **23**, 1557–1562 (2003).
167. Pape, H. C. Queer current and pacemaker: the hyperpolarization-activated cation current in neurons. *Annu. Rev. Physiol.* **58**, 299–327 (1996).
168. Robinson, R. B. & Siegelbaum, S. A. Hyperpolarization-activated cation currents: from molecules to physiological function. *Annu. Rev. Physiol.* **65**, 453–480 (2003).
169. McCormick, D. A. & Pape, H. C. Properties of a hyperpolarization-activated cation current and its role in rhythmic oscillation in thalamic relay neurones. *J. Physiol.* **431**, 291–318 (1990).
170. Maccaferri, G. & McBain, C. J. The hyperpolarization-activated current (Ih) and its contribution to pacemaker activity in rat CA1 hippocampal stratum oriens-alveus interneurones. *J. Physiol.* **497**, 119–130 (1996).
171. Wilson, C. J. & Callaway, J. C. Coupled oscillator model of the dopaminergic neuron of the substantia nigra. *J. Neurophysiol.* **83**, 3084–3100 (2000).
172. Stocker, M. Ca^{2+}-activated K^+ channels: molecular determinants and function of the SK family. *Nature Rev. Neurosci.* **5**, 758–770 (2004).
173. Pedarzani, P. *et al.* Specific enhancement of SK channel activity selectively potentiates the afterhyperpolarizing current I_{AHP} and modulates the firing properties of hippocampal pyramidal neurons. *J. Biol. Chem.* **280**, 41404–41411 (2005).
174. Gu, N., Vervaeke, K., Hu, H. & Storm, J. F. Kv7/KCNQ/M and HCN/h, but not KCa2/SK channels, contribute to the somatic medium after-hyperpolarization and excitability control in CA1 hippocampal pyramidal cells. *J. Physiol.* **566**, 689–715 (2005).
175. Lawrence, J. J. *et al.* Somatodendritic Kv7/KCNQ/M channels control interspike interval in hippocampal interneurons. *J. Neurosci.* **26**, 12325–12338 (2006).
176. Womack, M. D. & Khodakhah, K. Characterization of large conductance Ca^{2+}-activated K^+ channels in cerebellar Purkinje neurons. *Eur. J. Neurosci.* **16**, 1214–1222 (2002).
177. Edgerton, J. R. & Reinhart, P. H. Distinct contributions of small and large conductance Ca^{2+}-activated K^+ channels to rat Purkinje neuron function. *J. Physiol.* **548**, 53–69 (2003).
178. Vogalis, F., Storm, J. F. & Lancaster, B. SK channels and the varieties of slow after-hyperpolarizations in neurons. *Eur. J. Neurosci.* **18**, 3155–3166 (2003).
179. Bond, C. T. *et al.* Small conductance Ca^{2+}-activated K^+ channel knock-out mice reveal the identity of calcium-dependent afterhyperpolarization currents. *J. Neurosci.* **24**, 5301–5306 (2004).
180. Villalobos, C., Shakkottai, V. G., Chandy, K. G., Michelhaugh, S. K. & Andrade, R. SKCa channels mediate the medium but not the slow calcium-activated afterhyperpolarization in cortical neurons. *J. Neurosci.* **24**, 3537–3542 (2004).
181. Shah, M. M., Javadzadeh-Tabatabaie, M., Benton, D. C., Ganellin, C. R. & Haylett, D. G. Enhancement of hippocampal pyramidal cell excitability by the novel selective slow-afterhyperpolarization channel blocker 3-(triphenylmethylaminomethyl)pyridine (UCL2077). *Mol. Pharmacol.* **70**, 1494–1502 (2006).
182. Wong, R. K. & Prince, D. A. Afterpotential generation in hippocampal pyramidal cells. *J. Neurophysiol.* **45**, 86–97 (1981).
183. White, G., Lovinger, D. M. & Weight, F. F. Transient low-threshold Ca^{2+} current triggers burst firing through an afterdepolarizing potential in an adult mammalian neuron. *Proc. Natl Acad. Sci. USA* **86**, 6802–6806 (1989).
184. Jensen, M. S., Azouz, R. & Yaari, Y. Spike after-depolarization and burst generation in adult rat hippocampal CA1 pyramidal cells. *J. Physiol.* **492**, 199–210 (1996).
185. Swensen, A. M. & Bean, B. P. Ionic mechanisms of burst firing in dissociated Purkinje neurons. *J. Neurosci.* **23**, 9650–9663 (2003).
186. Metz, A. E., Jarsky, T., Martina, M. & Spruston, N. R-type calcium channels contribute to afterdepolarization and bursting in hippocampal CA1 pyramidal neurons. *J. Neurosci.* **25**, 5763–5773 (2005).
187. Haj-Dahmane, S. & Andrade, R. Calcium-activated cation nonselective current contributes to the fast afterdepolarization in rat prefrontal cortex neurons. *J. Neurophysiol.* **78**, 1983–1989 (1997).
188. Wong, R. K. & Stewart, M. Different firing patterns generated in dendrites and somata of CA1 pyramidal neurones in guinea-pig hippocampus. *J. Physiol.* **457**, 675–687 (1992).
189. Andreasen, M. & Lambert, J. D. Regenerative properties of pyramidal cell dendrites in area CA1 of the rat hippocampus. *J. Physiol.* **483**, 421–441 (1995).
190. Magee, J. C. & Carruth, M. Dendritic voltage-gated ion channels regulate the action potential firing mode of hippocampal CA1 pyramidal neurons. *J. Neurophysiol.* **82**, 1895–1901 (1999).
191. Williams, S. R. & Stuart, G. J. Mechanisms and consequences of action potential burst firing in rat neocortical pyramidal neurons. *J. Physiol.* **521**, 467–482 (1999). **Incisive analysis of the mechanism of all-or-none bursting in layer 5 pyramidal neurons, showing the crucial role of activation of dendritic sodium channels and calcium channels.**
192. D'Angelo, E. *et al.* Theta-frequency bursting and resonance in cerebellar granule cells: experimental evidence and modeling of a slow k^+-dependent mechanism. *J. Neurosci.* **21**, 759–770 (2001).
193. Achard, P. & De Schutter, E. Complex parameter landscape for a complex neuron model. *PLoS Comput. Biol.* **2**, e94 (2006).
194. Goldman, M. S., Golowasch, J., Marder, E. & Abbott, L. F. Global structure, robustness, and modulation of neuronal models. *J. Neurosci.* **21**, 5229–5238 (2001). **Remarkable demonstration — using modelling together with dynamic clamp experiments — that nearly identical bursting behaviour can be produced by highly variable combinations of levels of five conductances, even when small changes in a given conductance can modulate firing.**
195. Golowasch, J., Goldman, M. S., Abbott, L. F. & Marder, E. Failure of averaging in the construction of a conductance-based neuron model. *J. Neurophysiol.* **87**, 1129–1131 (2002).
196. Marder, E. & Goaillard, J. M. Variability, compensation and homeostasis in neuron and network function. *Nature Rev. Neurosci.* **7**, 563–574 (2006).
197. Swensen, A. M. & Bean, B. P. Robustness of burst firing in dissociated purkinje neurons with acute or long-term reductions in sodium conductance. *J. Neurosci.* **25**, 3509–3520 (2005).
198. Sharp, A. A., O'Neil, M. B., Abbott, L. F. & Marder, E. Dynamic clamp: computer-generated conductances in real neurons. *J. Neurophysiol.* **69**, 992–995 (1993).
199. Robinson, H. P. & Kawai, N. Injection of digitally synthesized synaptic conductance transients to measure the integrative properties of neurons. *J. Neurosci. Methods* **49**, 157–165 (1993).
200. Prinz, A. A., Abbott, L. F. & Marder, E. The dynamic clamp comes of age. *Trends Neurosci.* **27**, 218–224 (2004).
201. Goldman, L. & Schauf, C. L. Inactivation of the sodium current in *Myxicola* giant axons. Evidence for coupling to the activation process. *J. Gen. Physiol.* **59**, 659–675 (1972).
202. Aldrich, R. W., Corey, D. P. & Stevens, C. F. A reinterpretation of mammalian sodium channel gating based on single channel recording. *Nature* **306**, 436–441 (1983).
203. Vandenberg, C. A. & Bezanilla, F. A sodium channel gating model based on single channel, macroscopic ionic, and gating currents in the squid giant axon. *Biophys. J.* **60**, 1511–1533 (1991).
204. Kuo, C. C. & Bean, B. P. Na^+ channels must deactivate to recover from inactivation. *Neuron* **12**, 819–829 (1994).
205. Serrano, J. R., Perez-Reyes, E. & Jones, S. W. State-dependent inactivation of the alpha1G T-type calcium channel. *J. Gen. Physiol.* **114**, 185–201 (1999).
206. Beck, E. J., Bowlby, M., An, W. F., Rhodes, K. J. & Covarrubias, M. Remodelling inactivation gating of Kv4 channels by KChIP1, a small-molecular-weight calcium-binding protein. *J. Physiol.* **538**, 691–706 (2002).

Acknowledgements

I am grateful to M. Puopolo, M. Martina, B. Carter and A. Swensen for permission to use their unpublished data, and to them, Z. Khaliq and A. Jackson for much helpful discussion. Supported by the National Institute of Neurological Diseases and Stroke (NS36855).

Competing interests statement

The author declares no competing financial interests.